AAEC/E188

AAEC/E188

AUSTRALIAN ATOMIC ENERGY COMMISSION

RESEARCH ESTABLISHMENT
LUCAS HEIGHTS

ATOMIC DIFFUSION IN CERAMIC OXIDES

by

H.J. de BRUIN
D.H. BRADHURST
D.G. WALKER

December 1967

AUSTRALIAN ATOMIC ENERGY COMMISSION

RESEARCH ESTABLISHMENT

LUCAS HEIGHTS

ATOMIC DIFFUSION IN CERAMIC OXIDES

by

H. J. de BRUIN
D. H. BRADHURST
D. G. WALKER

ABSTRACT

Diffusion mechanisms in ceramic oxides are considered and available data in the literature broadly reviewed. It is noted that a simple correlation for cation self-diffusion in oxides based on structural considerations is not likely to eventuate, although some correlation for oxygen diffusion should exist. Greater sensitivity is required to study diffusion in oxides than can be obtained by conventional tracer lapping. The less common methods that may be applicable are reviewed.

This paper was presented at the Symposium on Properties of Materials at High Temperatures, sponsored by the Commonwealth Scientific and Industrial Research Organisation, Division of Mineral Chemistry, at North Ryde, N.S.W. on 21st and 22nd August, 1967.

CONTENTS

(continued)

CONTENTS (continued)

1. INTRODUCTION

Many of the properties and much of the behaviour of solids can be related to atom movements within the material during which atoms change from one rest position to another. Neglecting nuclear processes, in which the energies involved are very large, these movements fall into two classes: processes in which groups of atoms move in a co-operative manner and processes in which the atom movements are individual and uncoordinated. The former are frequently called shear processes and the latter diffusion processes.

The predominance of diffusion in most systems explains the importance of diffusion studies as a basis for understanding solid state behaviour. This has long been recognised by metallurgists and a considerable volume of diffusion data exists for metallic systems. However, with ceramic oxides, only limited studies have been made, although diffusion-controlled processes are of prime importance in the fabrication and utilization of these materials. Some illustrative examples of such processes are given below.

1. Sintering has been studied extensively by correlating the shrinkage of ceramic specimens with diffusion coefficients of the slowest moving ions. Kuczynski's original model[1], shown in Figure 1, still forms the basis of current sintering theories. Vacancies diffuse from the surface of spherical grains to the boundaries between them, via the bulk or along the surface. This gives rise to a decrease of the centre-centre distance and to neck formation as shown. The shrinkage can then be related to the diffusion coefficient in a variety of ways, depending on the diffusion mechanism. For example the simple expression by Kingery and Berg[2] suggests that for a bulk diffusion mechanism the relative shrinkage is inversely proportional to the temperature and the cube of the average grain size, and directly proportional to $(\text{time})^{2/5}$.

2. Phase transformations. Although many polymorphic changes occurring in pure ceramic oxides are now thought to be shear or martensitic in nature, diffusion-controlled phase changes are still of considerable importance in multi-component systems. For example, the use of an alumina coating on beryllia, as a protection against water vapour corrosion at elevated temperatures, has been discussed by Reeve[3]. At sufficiently high temperatures, the formation and growth of a chrysoberyl reaction layer by inter-diffusion may limit the life of the coating.

A special case of phase transformation which involves chemical change is oxidation of metals. In many cases, the reaction proceeds by the formation of an adherent oxide layer and can then only proceed by transport of either oxygen or metal through the oxides. This diffusion step is often rate-controlling and it can then be shown that the rate of increase in the thickness of the oxide layer will be inversely proportional to the thickness[4]:

$$\frac{dx}{dt} = \frac{k}{x} \qquad (1)$$

This leads to the well-known parabolic rate law:

$$x^2 = 2kt \quad , \qquad (2)$$

where x may be identified with the specific weight gain of the specimen. When more complicated diffusion mechanisms are operative, logarithmic, linear or cubic rate laws can be derived.

3. Diffusion-controlled deformation processes. Unlike metals, ceramic oxides rarely show any ductility at low temperatures ($< T_m/2$) even as single crystals. The reason in general is that resistance to dislocation movement is too great to allow significant slip to occur. Further, even if slip can be activated at sufficiently elevated temperatures, polycrystalline ceramic oxides show negligible slip ductility because the number of slip systems available never reaches the total of five necessary to maintain grain boundary coherence in a random polycrystalline aggregate.

However, as the temperature is increased until significant self-diffusion can occur, deformation by creep takes place, and, at sufficiently high temperatures, this can lead to surprisingly large strains. There would seem to be two main possibilities: diffusional creep and diffusion-controlled

creep. In the case of diffusional creep the diffusion itself creates the strain. Because the creation of a vacancy leads to an increase in the volume of a sample, a tensile stress will do work during vacancy formation and a compressive stress will do work during vacancy loss. Thus there will be an excess of vacancies over those at thermal equilibrium in regions of tensile stress, and the reverse for regions of compression. This will create a net flux of vacancies from tensile to compressive stress regions, that is, the specimen will elongate along the tensile axis.

During diffusion-controlled creep some other mechanism is responsible for the deformation, but diffusion – that is, the formation and supply of vacancies – is the rate-controlling factor. For metals several dislocation mechanisms and grain-boundary-sliding mechanisms of this kind have been postulated.

For ceramic materials generally neither the creep data nor the diffusion data are sufficiently accurate to allow the various mechanisms to be unequivocally resolved.

Yet, until some fifteen years ago, the subject of diffusion in ceramic oxides was neglected. There were a number of reasons for this:

1. Relatively high temperatures are required to study thermal diffusion in ceramics. Assuming that chemical compatibility problems can be overcome, it is not hard to achieve high temperatures, but to control and measure them precisely to within a few degrees over an extended period of time is still an arduous task. For example, conventional thermoelectric measurements can readily be made up to 1500 °C; thermocouples have just become available up to about 2500 °C, but beyond that temperature a good deal of guesswork, characteristic of radiative procedures, still prevails.

2. The physical and chemical quality of specimens leaves much to be desired. Besides problems of stoichiometry, which are absent in metals, single oxide crystals are still collectors' items. They contain relatively large amounts of impurities introduced during production. In polycrystalline specimens, which are hardly ever of theoretical density, several diffusion mechanisms operate simultaneously and are hard to evaluate separately.

3. If cation diffusion can be estimated, such studies only produce half of the self-diffusion picture. The absence of suitable oxygen radioisotopes necessitates the development of unconventional tracer techniques to attain a complete solution to the self-diffusion problem. Considerable doubt still exists about the validity of many oxygen diffusion data.

The first significant cation diffusion studies were published in 1949 by Moore [5] (Cu_2O) and in the early fifties by Lindner and co-workers (CaO & Fe_2O_3 [7], ZnO and spinels [8]) and Reddington [9] (BaO). The isotopic exchange method for the study of oxygen diffusion was pioneered by Haul [10] and co-workers in 1953.

In this paper we do not elaborate on the mathematics and physical fundamentals of the classical diffusion theory. Several textbooks [11] cover the quantitative aspects and many excellent reviews [12] have appeared in recent years. We consider the mechanisms of diffusion and point to the increased complexity of diffusion in ceramic oxides. A survey of the available literature seems appropriate, but this will be done in rather general terms, looking for correlations in cation and anion diffusion data. Because such correlation is not obvious we advocate the application of less common techniques for studying diffusion with greater sensitivity and higher accuracy. Some of these methods are reviewed.

2. DIFFUSION MECHANISMS

2.1 In Single Crystals

2.1.1 Volume diffusion

Some 90 per cent of papers devoted to the determination of diffusion parameters in metals as well as oxides, explain quantitative data in terms of simple bulk diffusion mechanisms, in which a migrating atom passes an energy barrier at the position of the activated complex before coming to rest in its final position.

Rarely, however, does one have the ideal lattice, even in a single crystal, where the kinetics of migration are not complicated by contributions of dislocations, grain boundaries, impurities and evaporation. In the ideal monatomic metal, lattice diffusion takes place via the migration of vacancies or via interstitial positions in the lattice. These mechanisms have all been adequately described in most previous reviews [12].

In ceramic oxides bulk diffusion also takes place by migration of point defects, but the nature of the defects is more complicated because electrical neutrality must be maintained. Ion vacancies are associated with the opposite ion vacancies (Schottky defects) or with their own interstitials (Frenkel defects), all of which are mobile at elevated temperatures. Furthermore, cations which can exist in several oxidation states or can vary their coordination number often give rise to non-stoichiometry, which must greatly affect diffusion rates, particularly those for oxygen.

An example of the more complex diffusion paths for cations through an oxide lattice is shown in Figure 2. In this rather naive physical picture the oxygen ions in a closest packed hexagonal oxide lattice have been removed, to emphasize the void space in between. For further clarity the voids are shown in an exploded fashion, assuming the ions to be hard spheres.

There are 4 different types of voids. Triangular voids (shaded) occur in the planes of closest approach of 3 oxygen ions; the cations must move through several triangles during a diffusion jump. Two types of tetrahedral voids occur and these are mirror images of each other. Octahedral voids in an hcp lattice form open channels in the $\underset{\sim}{c}$ direction.

From this figure one can draw several conclusions about cation bulk diffusion in an hcp oxide:

1. Interstitialcy, in which an interstitial atom dislodges another atom at a normal lattice site, is not a favoured mechanism because the required linear jump paths are usually obstructed.

2. Diffusion by the rotation of a ring of identical atoms, as is possible in monatomic systems, is excluded in binary compounds.

3. Diffusion by a vacancy mechanism is more complex than in monatomic systems and does not take place in a linear fashion. The energy diagrams show several activated complexes at the centres of the triangular voids.

Similar physical pictures can be drawn for other closest packed and more complicated crystallographic arrangements, in order to derive conclusions about bulk diffusion mechanisms.

2.1.2 Other mechanisms

Simple bulk diffusion is often complicated by other more rapid transport processes. Failure to acknowledge this fact could explain the breakdown of transport models for processes such as sintering, creep and grain growth.

The brittle nature of most ceramic single crystals reflects the immobility of dislocations which can act as high diffusivity paths. Dislocation densities can be quite substantial, and as a consequence one observes a depression of the values for Q and D_o in the Arrhenius expression for the diffusion coefficient:

$$D = D_o \exp(-Q/RT) \quad (3)$$

Zener [13] elaborated on the range of values for D_o for bulk self-diffusion and impurity diffusion by an interstitial or vacancy mechanism in metals. He postulated that the energy of migration is associated with lattice strain as the diffusing atom moves through the saddle point, and showed that the entropy change ΔS for bulk diffusion is always positive. From the theory of reaction rates [14] it can be shown that:

$$D_o = \lambda^2 \frac{k\theta}{h} \exp(\Delta S/R + 1) \quad , \tag{4}$$

where λ is the jump distance, which is of the same order of magnitude as the lattice parameter, θ is the Debye temperature, and k, h and R have their usual significance. For bulk diffusion in ceramic oxides, that is, for positive values of ΔS, D_o should be greater than 10^{-2} cm^2/sec. When other rapid diffusion mechanisms are operative, such as pipe diffusion, the entropy change becomes negative and substantially lower pre-exponentials are obtained. Harding [15] used such observations to criticize an alleged correlation between the activation energy for impurity diffusion in MgO and the ratio of ionic radius to the polarizability of the impurity ion [16,17]. He pointed to values for D_o between 10^{-4} and 10^{-5} cm^2/sec at low temperatures compared with values between 10^{-2} and 10 cm^2/sec at high temperatures, and warned against attributing too much significance to the values of the activation energies for impurity diffusion, when the pre-exponential values are too low.

Dislocations in an ionic crystal will further enhance bulk diffusion because of the electrostatic charge which is commonly associated with them [18]. Such fields are conducive to the formation of extrinsic defects which again will decrease apparent activation energies and increase diffusion rates.

The presence of an impurity of higher valence than that of the cation will also have the same effects as the presence of dislocations, but its contribution can often be estimated from chemical analyses.

2.2 Polycrystalline Specimens

Unfortunately single crystals of ceramic oxides are hard to obtain and many investigations on transport in these oxides have been carried out on polycrystalline specimens. These studies are complicated by two main factors: diffusion along grain boundaries (which are regions of high disorder), and the effects of low density on mass transport.

Grain boundary diffusion in ceramic oxides is not different in principle from the same phenomenon in polycrystalline metals. It has received relatively little attention although its contribution to transport-dependent processes such as creep and sintering is well realized.

The effects of grain boundaries on diffusion are clearly apparent in the penetration profiles of tracers into inactive specimens, as shown for ^{7}Be into BeO in Figure 3. The relative concentration of the Be tracer should vary directly as the square of the distance for bulk diffusion, but at some distance into the specimen it is proportional to the first power of the penetration, a feature characteristic of diffusion along the grain boundaries [19].

The effect on the temperature dependence of the diffusion coefficient is again a lowering of both activation energy and pre-exponential (in Equation 3).

The effects of transport via grain boundaries are relatively small if diffusion is studied at high temperatures as in the case of pipe diffusion. These effects can be further minimised by using polycrystalline specimens with as large a grain size as possible. A useful empirical criterion to remember is the observation that if the coefficient for diffusion along grain boundaries is significantly greater than that via the bulk (say $D_g/D_b > 10^3$), the grain size (r) should be at least twice the average diffusion length:

$$(2 D_b t)^{1/2} < r/2 \quad , \tag{5}$$

in order to neglect diffusion via the boundaries. Several reviews on grain boundary diffusion in metals are available [19]. The basic theory is also applicable to diffusion in ceramic oxides.

Little effort has been made to study the effects of the relatively low densities of polycrystalline specimens on the diffusion process. Rarely is their density greater than 98 per cent of theoretical. The usual range is 95 to 97 per cent and in some cases as low as 91 per cent.

The possibility of migration via open channels with critical dimensions several orders of magnitude larger than those of grain boundaries or dislocations has only been investigated quantitatively for cation diffusion in low density beryllium oxide [20]. Figure 4 shows the effects on the concentration profiles for the penetration of ^{7}Be into BeO as the density decreased from near theoretical to 75 per cent, for constant conditions of time and annealing temperature. It is clear that the contribution of a very rapid diffusion process through the intergranular space is quite pronounced. The mechanism postulated depended on a number of processes taking place simultaneously:

1. Evaporation – condensation.
2. Exchange equilibria between a vapour phase and the sintered surface.
3. Knudsen diffusion through the pores.
4. Volume diffusion into the matrix, away from the pores.
5. Diffusion along the surface of the grains.

No simple interpretation can be derived on theoretical grounds, but the geometry for this rapid diffusion process was not unlike that for migration via grain boundaries and a modified Fisher [19a] model was applied to data with reasonable success. The derived diffusion coefficients are shown in Figure 5. If one can accept the scatter of the data in the light of the simplifying assumptions, the activation energy was found to be 139 ± 20 kcal/mole. This is close to the value [21] for the heat of sublimation of BeO (150 ± 5 kcal/mole).

These findings could be of significance in the interpretation of transport-dependent properties such as sintering and grain growth, where migration other than via the bulk could conceivably take place. Aitken [22], using a similar model to that in Figure 1, found an activation energy of approximately 150 kcal/mole.

Basically there is no difference in the application of Fick's principles to migration in the solid state, whether the medium consists of a metallic or a ceramic lattice. In its simplest form diffusion through a homogeneous medium is described by a differential equation:

$$\frac{\partial C}{\partial t} = D \Delta C \quad , \tag{6}$$

where Δ is Laplace's operator, $\partial^2/\partial x^2 + \partial^2/\partial y^2 + \partial^2/\partial z^2$, and the diffusion coefficient D can be a constant, or a function of any of the variables time t, concentration c, or the spatial coordinates x, y, and z. The solutions of this equation, and consequently the interpretation of experimental data, are decided by geometry and the mechanisms by which migration takes place. Basic diffusion theory, however, has been covered adequately elsewhere [11, 12].

3. REVIEW OF LITERATURE DATA

Criticism of literature data in this review is confined essentially to the problems of self-diffusion.

Some 200 papers have appeared containing quantitative self-diffusion data in ceramic oxides. Several reviews [23] evaluate these data critically. We do not elaborate exhaustively on individual findings, but rather look for some general trends which may help to bring some system into a collection of apparently unrelated data. The bibliography by Cumming and Harrop [24] is a useful summary of the findings of many workers until 1965. Although many papers have appeared since, the bibliography serves as a handbook in the investigation of the existence of possible correlations; individual papers have to be consulted to evaluate data appropriately.

So far no empirical relations similar to those found for self-diffusion in metals have been proposed to describe diffusion parameters in oxides. A number of such relations as they apply to diffusion in metals are listed below:

$$Q = 1.48 \times 10^{-3}\ T_m \text{ eV (Ref. 25)} \quad (7)$$

$$= 34\ T_m \text{ kcal/mole (Ref. 25)}$$

$$Q = 38\ T_m \text{ kcal/mole (Ref. 26)} \quad (8)$$

$$\log D \text{ (at melting point)} \approx -7 \text{ (Ref. 27)} \quad (9)$$

$$\approx -9 \text{ for alkali halides (Ref. 28)}$$

$$\approx -8 \text{ for substitutional impurity diffusion in metals (Ref. 11b)}$$

$$Q = 0.64\ L_S \text{ (Ref. 11b)} \quad (10)$$

$$Q = 16.5\ L_m \text{ (Ref. 29)}, \quad (11)$$

where T_m is the melting point in absolute degrees, L_S is the latent heat of sublimation and L_m is the latent heat of fusion.

None of the expressions for the activation energies seem to have any foundation when applied to cation diffusion in oxides. This is not entirely unexpected. For cation diffusion in ceramic oxides an equivalent for Equation 9 does not exist, and diffusivities vary over some 5 orders of magnitude between 10^{-11} and 10^{-6} cm^2/sec.

Structurally most metals fall within fewer than six well-defined classes; they are held together by simple metallic bonds and nuclear dimensions can be accurately determined. Virtually none of these conveniently ordered properties apply to cations in oxides. Their diatomic characteristics give rise to many more crystallographic arrangements, often further complicated by phase changes below their melting point. We refer to these compounds as ionic, but realize that none of them are entirely ionic. The degree of covalence varies considerably between oxides and is hard to quantize. Consequently, polarization and nuclear dimensions of the ions are equally hard to estimate. With the subject as new as it is, an attempt to correlate the available data seems premature.

However, some correlation should be apparent in the diffusion behaviour of the common ion in oxides. Figure 6 is a summary of oxygen diffusion data in hexagonal and cubic oxides. Not all the data published are shown, but the summary does serve some useful purpose by suggesting the following generalizations:

1. Oxygen diffusion coefficients at the melting points of the oxides seem to fall in a broad band around 10^{-10} cm^2/sec.

2. Activation energies for hexagonal oxides are greater than those for cubic oxides and these are greater than for tetragonal oxides:

$$Q_{hex} > Q_{cub} > Q_{tetr}$$

These are by no means steadfast rules; there are many exceptions.

It is obvious, however, that one cannot be confident about the current published data when attempting a serious correlation on diffusion in oxides, because:

(a) Much data has been obtained by indirect means. Sintering, creep and oxidation mechanisms are not sufficiently understood to derive accurate diffusion data. In sintering, for example, it is more than likely that transport mechanisms such as evaporation – condensation and surface and grain boundary diffusion obscure clear cut bulk migration models.

(b) Many of the published data show pre-exponentials which are so low that they cannot be justified by the theory of atomic diffusion. In those cases rapid transport paths must be operative. One outstanding example is the diffusion of chromium in chromic oxides as shown

in Table 1. Activation energies are correspondingly affected. Oxygen diffusion in Al_2O_3 [30], BeO [31], PbO [32], MgO [33], NiO [34], SiO_2 [35] and TiO_2 [36] at temperatures well below the melting point also suggest rapid migration mechanisms.

Current trends in the determination of diffusion parameters in ceramic oxides are concentrated on improving the experimental approach. Specimens require better characterization and methods are needed which are more sensitive than the tracer lapping technique for cations and mass spectrometry of atmospheres for oxygen diffusion. In the next sections we therefore elaborate on some of the more promising techniques which could be applied to a quantitative study of diffusion in oxides.

4. EXPERIMENTAL DETERMINATIONS

The determination of cation diffusion parameters in ceramic oxides is popular, while reliable information on oxygen diffusion is restricted because of the limited and rather cumbersome techniques that are available to study the penetration of oxygen. The large range of radioisotopes, even those of relatively short half lives, make tracer lapping experiments very attractive. This standard technique is extremely popular and has been reviewed on many occasions [12].

In this paper we restrict ourselves to the less common methods involving the use of radiotracers in which, because of the relatively small sensitivity that can be obtained from grinding ceramic specimens compared with metals, accurate removal of thin layers from the specimen is not a criterion. The minimum thickness of layers that can be removed accurately from the brittle and inert ceramic specimen is at least an order of magnitude larger than that for most metals. Consequently the minimum average diffusion length, $(2\,Dt)^{1/2}$, must be at least 15 to 20 μm in ceramics compared with often less than 1 μm in metals. In practice this means working at higher temperatures and for longer times.

As pointed out, the problems of control at higher temperatures give rise to greater errors in the derived parameters. If the uncertainty in temperature is Δ_T then the probable error in the diffusion coefficient [40] is:

$$\Delta_D = \frac{Q}{RT}\Delta_T \quad . \tag{12}$$

For Δ_T = 0.5 per cent at 1500 °K and an activation of 100 kcal/mole, $\Delta_D \simeq 17$ per cent, a fluctuation of $\pm 8°$ at 1500 °K over a period of several weeks is not excessive. During the determination of diffusion coefficients by lapping procedures, these considerations set the lower limit at about 10^{-12} to 10^{-13} cm^2/sec.

4.1 Cation Diffusion

4.1.1 Molten salt exchange method

Savitsky's method [41] of isotope transfer from a molten salt seems well suited for the determination of cation diffusion coefficients in ceramic oxides when only very small single crystals are available. A sensitivity of 10^{-20} cm^2/sec is claimed for metals and since the method does not involve any destructive analysis of the specimen, such as lapping, there is no reason why this sensitivity cannot be achieved with ceramic oxides. An inactive oxide specimen is suspended in a molten salt with a common cation. The salt is spiked with an appropriate isotope and if one can assume perfect compatibility, and a virtually instantaneous exchange at the ceramic surface, then the increase in activity will be proportional to the square root of time:

$$\frac{I - I_o}{I_o} = \frac{2d}{\sqrt{\pi}}\sqrt{Dt} \quad , \tag{13}$$

where I is the activity after an anneal lasting t seconds, I_o is the activity adsorbed on the surface and d the thickness of this adsorbed layer. If the exchange is rapid, I_o can be determined and d is postulated to be the interatomic distance.

4.1.2 The "imprint" method

When a thin tracer deposit on one side of the ceramic diffuses into the specimen the concentration (activity) at any depth can be obtained from the Gaussian solution of the diffusion equation:

$$C(x,t) = \frac{M_o}{(\pi Dt)^{1/2}} \exp\left(\frac{-x^2}{4Dt}\right) \quad , \tag{14}$$

where M_o is the amount of tracer deposited. When $x = 0$ this becomes:

$$C(0,t) = \frac{M_o}{(\pi D)^{1/2}} \cdot \frac{1}{t^{1/2}} \quad . \tag{15}$$

Thus if M_o remains constant the surface activity should be inversely proportional to the square root of time. However in order to obtain a diffusion coefficient from the slope of such a curve it is essential to know the relation between concentration and the count rate of the tracer, as well as the absorption coefficient of the ceramic for the particular type of radiation. This information can be obtained by standard radiochemical procedures.

The determination of the absorptive properties can be avoided if an exchange equilibrium is established rapidly between the ceramic surface and an aqueous solution of the cation.

The exchange, for example, between an aqueous solution of a ^7Be tracer and an inactive highly sintered BeO specimen has been found to be a convenient method of depositing tracer activity on the ceramic compact [43]. It has since been found that this method also applies to depositing ^7Be on Al_2O_3 [44]. Very little information is available on the exchange between highly sintered ceramics and aqueous solutions, but there is no reason to believe that such exchange does not take place in many of these instances. The exchange reaction under appropriate conditions of pH and concentration is reversible. This technique can be applied to 'fingerprint' active surfaces of a ceramic specimen and makes it possible to use the so-called 'imprint' method [42] on ceramics, with the possibility of determining diffusion coefficients as low as 10^{-15} cm^2/sec in substantially shorter annealing times.

4.1.3 Methods based on the absorption of radiation

Methods based on the absorptive properties of the ceramic for soft nuclear radiation can be adapted to avoid the lack of sensitivity inherent in the rather rough lapping procedures. If a layer of the cation tracer is deposited on one side of a specimen of thickness ℓ, as shown Figure 7, then as diffusion proceeds the activity measured at Side 1 will decrease and that on Side 2 will increase. The change in activity on both sides will depend on the tracer diffusion rates and the absorptive properties of the medium.

Gainotti and Zecchina [45] measured the relative increase in activity on Side 2 as a function of time and this is given by:

$$\frac{I_2}{I_2^0} = \exp(\mu^2 Dt)\left\{ \operatorname{erf}\left[\frac{1}{(4Dt)^{1/2}} - (\mu^2 Dt)^{1/2}\right] + \operatorname{erf}(\mu^2 Dt)^{1/2}\right\} \quad , \tag{16}$$

where μ is the absorption coefficient of the medium for the measured radiation. For sufficiently short times when $(\mu^2 Dt)^{1/2} << 1$ and with the thickness ℓ such that $1/(4Dt)^{1/2} > 3$ this approximates to:

$$\frac{I_2}{I_2^0} = 1 + 2\mu\left(\frac{Dt}{\pi}\right)^{1/2} + \mu^2 Dt \quad , \tag{17}$$

from which D can be obtained if μ is known.

If the tracer emits both γ and β rays, advantage can be taken of the difference between the relatively large value of μ_β and the value of μ_γ [46]. It is then not necessary to work with thin specimens, and it can be shown, by measuring the decrease of both β and γ activity with time, that:

$$\frac{I_\beta(t)}{I_\beta(0)} \Big/ \frac{I_\gamma(t)}{I_\gamma(0)} = \exp(\mu_\beta^2 Dt) \{1 - \text{erf} [\mu (Dt)^{1/2}]\} , \qquad (18)$$

where $I_\beta(t)$ is the β activity at the surface after an anneal lasting t seconds, and $I_\beta(0)$ this value at the beginning of the experiment. The significance of the other symbols is obvious.

For monochromatic radiation μ can be determined experimentally by applying the exponential decay of the activity with depth:

$$\frac{I(x)}{I(0)} = \exp(-\mu x) \quad . \qquad (19)$$

This method can be cumbersome if the radiation exhibits a complex spectrum of energies.

Zhukhovitzky [40] showed that it was not essential to know the absorption characteristics if one counted both sides of the specimen at time intervals. He showed by solving Fick's law that:

$$\ln \left(\frac{I_1 - I_2}{I_1 + I_2} \right) = \ln K - mt \quad , \qquad (20)$$

where K is an expression containing absorptivity and diffusivity parameters, which do not have to be known in this simple linear expression in t, and

$$m = \frac{\pi^2 D}{\ell^2} , \qquad (21)$$

from which D can be determined.

These methods have not been applied to ceramic oxides, but they show great promise in the investigation of transport in oxide layers connected with corrosion of metals. Thin specimens can be obtained by chemically stripping the metal. The thickness of the specimen depends largely on two conditions, namely the energy of the measured radiation and the thickness of the tracer deposit. For a 1 μm deposit of a 0.5 MeV β emitter, ℓ should be between 30 and 100 μm.

The difficulties of preparing thin specimens have been avoided in another method by Zhukhovitzky [47] based on the absorptive properties of the medium, where semi-infinite geometry is assumed. However the determination of activity at infinite time by homogenizing a specimen is at least very cumbersome and long annealing times are required. These methods have been reviewed recently [48].

4.1.4 Isotope effects

One of the most powerful methods of establishing the diffusion mechanism in a particular migration problem is to study the rates at which different isotopes of an appropriate element diffuse under identical conditions [52].

For most applications the assumption that the tracer diffusion coefficient is identical to the atomic diffusion coefficient is valid to within the experimental errors involved in the interpretation of tracer diffusion data. Atomic diffusion by any mechanism is a perfectly random event. However, the probability that a labelled atom will move in a particular direction is correlated to previous jumps and is not entirely random, if kinetics of order greater than unity are involved as shown in the monatomic system in Figure 8. In ceramic oxides actual jumps are more complicated but the statistical inferences are the same. As indicated before, only vacancy and interstitial mechanisms need be considered here.

Kinetically an interstitial jump is a first order rate process. The labelled atom in a and b has an equal probability of jumping in any of the 4 directions indicated. The process is perfectly random; there is no difference between atomic and tracer diffusion. In the vacancy mechanism, however, the kinetics are of higher order if the jumping atom is a labelled one. That is, the movement of the tracer depends on the concentrations of labelled atoms and of vacancies. For atomic diffusion by vacancy drift the concentration of atoms is so great that migration is a function of vacancy concentration only. After the jump shown in c has taken place the probability that the labelled atom in d jumps back to its original position is far greater than movement in any other direction even in the presence of other vacancies nearby. The tracer diffusion coefficient is smaller than the atomic diffusion coefficient. If we define

$$f = \frac{D_t}{D_a} \quad , \tag{22}$$

then for a particular crystal structure this correlation factor can be derived by comparing the statistical jump probabilities of the labelled atoms with those of the host atoms. For vacancy diffusion in an hcp lattice Mullen[49] showed f to be 0.783, and in fcc and bcc lattices LeClaire[12b] used f = 0.7815 and 0.7215 respectively. Compaan and Haven[50] calculated f for a number of ionic crystals. For a direct interstitial mechanism f = 1 as is shown in Figures 8a and 8b.

Schoen[51] related the diffusion rates of two isotopes of the same element in a host medium to their mass ratio by the simple equation:

$$\left(\frac{D_1}{D_2} - 1\right) = f\left[\left(\frac{m_2}{m_1}\right)^{1/2} - 1\right] \tag{23}$$

Thus by determining the diffusion coefficients of the isotopes simultaneously, f can be obtained and some pertinent conclusions drawn about possible diffusion mechanisms.

Using the tracer lapping method for an experiment such as the above in which one determines the activity of both isotopes at any depth x after a diffusion anneal, it is simple to show that the logarithm of the activities must be proportional to the square of the penetration distance:

$$\ell n\ I \propto \left[-\frac{x^2}{4Dt}\right] \tag{24}$$

Thus, for the ratio of activities of the isotopes,

$$\ell n\ \frac{I_1}{I_2} = A - \frac{x^2}{4t}\left\{\frac{1}{D_1} - \frac{1}{D_2}\right\}, \tag{25}$$

where A is a constant. Hence

$$\ell n\ \frac{I_1}{I_2} = A' + \ell n\ I_1\left(\frac{D_1}{D_2} - 1\right) \quad . \tag{26}$$

It is thus unnecessary to know the depth of penetration accurately. By simply plotting on a log-log scale the ratio of the activities of each isotope versus that of one of them, the term $D_1/D_2 - 1$ can be obtained and f determined.

The criterion for a successful experimental determination is the choice of suitable isotopes, and the following points must be considered.

1. Their radiations must be different enough to allow individual determination. Thus γ counting for one and β counting for the other, or spectrometry of the radiation energetics, or even half-life determinations can all be used.

2. The half-lives of the isotopes must be long enough to allow adequate time for a diffusion anneal. A reasonable profile is obtained when the average diffusion length is approximately

25 microns ($= (2Dt)^{½}$). If the diffusion coefficient is 10^{-9} cm^2/sec, the anneal needs to last 1 hour. If $D = 10^{-12}$ cm^2/sec, the anneal is spread over 5 weeks. Allowing for handling of the isotope and analysis of the specimen it is reasonable to put the half-life of the isotope at least equal to the annealing time. Thus, in the examples above, the half-life should be at least 1 hour for the very fast diffusion or 35 days at the slower rates.

3. The difference in mass between the isotopes must be sufficient to give measurably different diffusion rates. The value of $(m_2/m_1)^{½} - 1$ should be at least 0.020 for reasonable sensitivity.

In Table 2 we suggest a number of isotopes that can be used to advantage in determining mechanisms for self-diffusion or solute diffusion in ceramic oxides, a field which is wide open for extensive investigation. The table has been drawn up on the basis of the 3 considerations above. The isotopes shown are readily available. Only the system $^{7}Be/^{10}Be$ is being investigated to determine the self-diffusion mechanism in BeO and of impurity diffusion in Al_2O_3 and MgO.

Elements with a widespread spectrum of inactive, naturally occurring isotopes are of particular interest. On irradiation of natural tin, for example, one obtains a range of the most useful isotopes from mass number 113 to 125, and these can be applied without separation in an isotope effect experiment. Natural zinc and calcium are other examples that can be used to advantage.

4.1.5 Chemical diffusion

The phenomenon of chemical diffusion in ceramic oxides is another problem which has received relatively little attention; and yet an understanding of the processes that take place when two solids, either or both being a ceramic oxide, are in contact with one another at elevated temperatures, is of great practical importance. Oxidation of metals is essentially determined by chemical diffusion processes, particularly in the oxide layer. The performance of ceramic coatings on nuclear fuels is greatly influenced by mass transport at the interface, complicated by the effects of neutron irradiation. The general practice of influencing sintering and grain growth by the empirical addition of other oxides is based on assumptions of rapid homogenizing of the contacted phases by chemical diffusion either at the interface or in the bulk.

The complications in chemical diffusion are due to two innate conditions: the diffusion coefficients are not constants, but increase as concentration increases, and the diffusion of solid A into B usually takes place at a rate different from that of B into A , which results in a net flux of matter. This flux can be measured quantitatively by marking the initial interface, as in the experiments by Smiegelskas and Kirkendall[53], in such a way that it can be located after the diffusion anneal. To find the diffusion coefficient of each component as a function of concentration, the Matano-Boltzmann graphical method[54] can be applied, shown in Figure 9. The diffusion coefficient is not constant and Fick's second law must therefore be written:

$$\frac{\partial C}{\partial t} = \frac{\partial}{\partial x}\left(D \frac{\partial c}{\partial x}\right) \quad , \tag{27}$$

which has a unique solution if we introduce the variable $\lambda = xt^{-½}$. It is then simple to show that any concentration

$$D(c) = -\frac{1}{2} \frac{\partial \lambda}{\partial c} \int_0^c \lambda dc \quad . \tag{28}$$

The term $\partial\lambda/\partial c$ is the gradient of the curve where the concentration is c , and the integral is the area under the curve. Solutions are available[55] to apply this method in the regions of extremely high and low concentrations, where gradients and areas under the curve have little meaning.

This chemical diffusion coefficient can be related to the individual coefficients D_A and D_B by means of the equations formulated by Darken[56] who showed that if the molar volume of the solid solution is constant,

$$D(c) = D_A X_B + D_B X_A \quad , \tag{30}$$

and

$$V = (D_B - D_A) \frac{\partial X_B}{\partial x} \quad , \tag{31}$$

where X_A and X_B are the mole fractions of A and B and V is the velocity with which the marked plane has travelled during the anneal. Having measured D(c) with respect to the marked plane by the Matano-Boltzmann method, and knowing the profiles of A and B and the distance this plane has travelled, these simultaneous equations can be solved.

With metals, Kirkendall shifts are studied by placing inert metal wires or fine-grained alumina at the interface. At the high temperatures where diffusion rates become measurable, it is not easy to find markers compatible with the ceramic oxides. This fact and the limited amount of information on phase diagrams of ceramics may account for the virtual lack of quantitative chemical diffusion data.

Holt and Condit [57] have recently suggested that if oxygen diffusion in the two ceramic oxides is negligible compared with their cation diffusion, an ^{18}O interface can be detected by proton activation and autoradiography as shown in Figure 10. This method is discussed in detail under oxygen diffusion. A diffusion couple with an ^{18}O layer in between is made by hot pressing at a temperature well below that for the proposed diffusion anneal. Half of such a specimen is annealed and the other half used to locate the original interface precisely. Both halves are cut at a low angle and the fresh surfaces irradiated in a proton accelerator, where

$$^{18}O\ (p,n)\ ^{18}F \quad . \tag{32}$$

The ^{18}F, which has a short half-life (112 mins), is a positron emitter which can readily be detected by autoradiography. The interface can thus be detected in both the annealed and blank specimens. To determine the cation concentration gradient, electron microprobe analysis can be used or even radiochemical methods if either specimen A or B was initially uniformly active.

Corrosion of metals is an extreme case of chemical diffusion, where, in addition to the solid-solid interface, the processes at the solid-gas interface are also important. The movement of a marker, originally deposited on the metal, as shown in Figure 11, may decide whether cation or anion diffusion through the oxide is the rate-determining process. The marker is usually an isotope of the metal being studied, but any tracer which does not interfere with the migration through the oxide can be used. If oxidation rates are determined by the rate at which the cation moves through the oxide, the tracer will essentially remain at the metal-oxide interface. However, if corrosion takes place by an oxygen diffusion mechanism the tracer will be displaced from the metal and remain at the oxide-gas interface.

The presence of a source of radiation under an oxide layer opens the possibility of using the absorptive properties of the radiation for the study of corrosion in terms of transport properties. The work by Cox and Roy [58], based on a method developed by Ollerhead et al. [59], and of Condit and Holt [60], could end the stalemate which seems to have been reached in corrosion by weight gain and metallography studies.

Cox and Roy [58] applied α spectrometry to the determination of the energy and number of α particles emitted in the reaction:

$$^{17}O\ (^3He,\alpha)\ ^{16}O \tag{33}$$

which has a Q value of 16 MeV. Specimens oxidized alternately in ^{17}O and ^{16}O atmospheres have an ^{17}O gradient. When bombarded with about 5 MeV ^3He ions, the energy of the emitted α particle depends entirely on the length of the path through the oxide layer. The energy loss of energetic secondary particles in accelerator reactions, which is caused by the stopping power of a compound, can be calculated quite accurately [61]. The number of α particles in this known spectrum of energies can therefore be translated into a ^{17}O concentration gradient from which diffusion parameters and mechanisms can be obtained. Applying this procedure to the oxidation of zirconium, Cox and Roy came to the conclusion that oxygen migration via boundaries and other rapid diffusion paths in the oxide layer is rate-determining and that oxygen bulk diffusion is too low to be detectable. From

their data it can be shown that this method has a sensitivity of better than 10^{-15} cm^2/sec for anneals lasting only a few hours. The proposed analytical method seems rather extravagant; the expensive ^{3}He ion source has the advantage of giving α particles of very high energy, but it does so also with ^{18}O (Q = 12.509, see Table 3) which is considerably cheaper than ^{17}O.

The method by Condit and Holt [60] makes it possible to investigate an earlier and perhaps more critical stage in the corrosion process, namely the initial growth of the oxide film immediately after nucleation. Cox's activation method is sensitive for oxide layers from about 5 x 10^3 Å to about 5 μm, and Condit's method is applicable for deposits from a few monolayers to about 10^3 Å.

The marker used is ^{228}Th, a 1.9 year α emitter, with short-lived decay products. Instead of measuring the α radiation of the decaying nuclide, Condit and Holt collected the recoiling radium daughter on a plate above the specimen. The range calculations for these relatively low energy recoil nuclei are very cumbersome and depend on parameters which are not accurately known. Friedlander and Kennedy [62] suggest empirical relations from which an approximate range can be calculated. For ^{224}Ra, the recoil energy E_{Ra} is calculated from E_α, the energy of the α decay of ^{228}Th (5.42 MeV):

$$M_{Ra}\, E_{Ra} = M_\alpha E_\alpha \quad , \tag{34}$$

where M_α is the mass of the α particle (y) and M_{Ra} that of the radium nucleus. (E_{Ra} = 97 keV). To calculate, say, the range R_{Zr} in zirconium (Z = 40, M = 91), one first obtains the proton range in zirconium (r_{Zr}) from the empirical relation [62]:

$$\frac{r_{Zr}}{r_a} = 0.90 + 0.0275\ Z + (0.06 - 0.0086\ Z) \log \frac{E_{Ra}}{M_{Ra}} \quad , \tag{35}$$

where r_a is the range in air of a proton of energy E_{Ra}/M_{Ra}, which can be obtained from the tables or graphs. The proton energy equivalent is 4.3 x 10^2 eV, and its range about 10^{-2} mg/cm^2 (Ref. 62, Figure 7-2); $r_{Zr} \cong 0.75\ r_a = 7.5 \times 10^{-3}$ mg/cm^2. Furthermore the value of R_{Zr} is related to r_{Zr} by:

$$R_{Zr} = \frac{M_{Ra}}{z^2}\ r_{Zr} \quad . \tag{36}$$

The value of z, which is the charge on the recoiling radium ion, is not exactly known. For the initial value of E_{Ra} a value of 4 to 5 is not unreasonable. Hence all recoil will be stopped within a layer of about 1000 Å; this is 2 to 3 times as high as the value experimentally determined by Condit [60]. Small corrections are required to apply such calculations to oxides but these are insignificant compared with the approximations implied.

4.2 Methods for Studying Oxygen Diffusion

4.2.1 Mass spectrometric methods

Of the four active oxygen isotopes, ^{15}O has the longest half life, 2.1 minutes. Methods for detecting oxygen transport are therefore all based on the detection of the stable isotopes ^{17}O and ^{18}O, which have a low abundance compared with ^{16}O. One either monitors the atmosphere (enriched in ^{17}O or ^{18}O), in which a specimen is being heated, by mass spectrometry, or determines the ^{17}O or ^{18}O gradient after the anneal by making use of some characteristic nuclear property of the less abundant isotopes (^{17}O ~ 0.037 per cent and ^{18}O ~ 0.20 per cent).

Several mass-spectrometric determinations for oxygen diffusion coefficients in ceramic oxides have been carried out. The $^{18}O_2/^{16}O_2$ peak is measured as a function of time and it is assumed that diffusion is the rate-determining step in the depletion of the enriched atmosphere. The data are processed by quite standard procedures (see for example Haul et al. [63] or Holt [64]). The disadvantages of this method are:

(i) The data obtained do not reveal the diffusion mechanisms. Even in powdered single crystals of ceramic oxides one must anticipate the presence of rapid diffusion paths such as dislocations.

(ii) The diffusion step is not necessarily rate-determining. In fact, the source of ^{18}O is extremely important in this regard. Exchange between O_2 and BeO [65] for example is very slow while that between CO_2 and BeO is considerably faster. Austerman [66] resolved these problems by lapping his specimens after an anneal in an enriched atmosphere, and determining the $^{18}O/^{16}O$ ratio in the grindings by vacuum fusion and mass spectrometry. However, the sensitivity of this method is considerably smaller.

4.2.2 Methods based on activation of oxygen isotopes

Currently several methods are being developed and these are based on the nuclear properties of the oxygen isotopes. After an anneal with a source enriched in ^{17}O or ^{18}O, the concentration gradients of these stable isotopes in the specimen are obtained and the specimen is then irradiated by nuclear particles of an appropriate energy. The concentration of the product nucleus, or the emission of secondary particles can be correlated with the original isotopic concentration in the specimens, from which a profile is then deduced.

Table 3 is a list of the most important nuclear reactions of ^{16}O, Table 4 gives those for ^{17}O, and Table 5 those for ^{18}O. Reactions with ^{16}O are useful for oxygen diffusion in metals, while those for ^{17}O and ^{18}O can be applied in studying ceramic oxides. These data were obtained from a publication by Ajzenberg et al. [67]. The Q value is the energy release of the particular reaction, not the threshold energy. Neither is it an indication of the cross section. It is the minimum energy of the particle accelerator required for the reaction. Thus if a 3 MeV positive particle accelerator is available, all reactions with $Q < -3$ MeV cannot be used.

Two procedures are used, depending on whether (i) the product nucleus after activation is radioactive, or (ii) the recoiling secondary particle has sufficient energy to emerge from the oxide.

In the first case the half life must be sufficiently long to permit detection. This restricts the choice to ^{14}C, a 5.76×10^3 year soft β emitter, and ^{18}F, a 112 minute positron emitter with a 0.51 MeV γ. The first is only formed in neutron activation which is not favoured in these analyses. Nearly all elements give active product nuclei on neutron activation and this interferes with the radio chemical analysis of ^{14}C. Furthermore secondary reactions due to recoil protons, deuterons, and so on, cannot be avoided. In this category only the $^{18}O\ (p,n)\ ^{18}F$ and $^{17}O\ (d,n)\ ^{18}F$ reactions, which have reasonable cross-sections, have been investigated [57, 68, 69].

In the second case the recoiling particle can be analysed during the activation process, this is similar to the method by Ollerhead et al. [59] described above. The choice of useful reactions in this group is considerably greater, particularly if one does not rely on the absorption properties of the emitted particle to reveal the depth of penetration by spectrometry. By cutting a wedge across the profile and allowing the ion beam to scan the exposed surface, a count of the particles of a known energy can be related to the concentration of the oxygen isotope. The reaction $^{18}O\ (p,\alpha)\ ^{15}N$ has been used to study oxygen diffusion in quartz [70,71]. However, there are usually several interfering reactions either in the specimen or with materials in the path between specimen and detector. Low count rates are a further disadvantage for such in-situ measurements. Specimens have to be counted for relatively long periods (5 – 15 minutes at each spot) and this demands great stability in the control of beam current and energy. Accelerators must become far more sophisticated to achieve these ideal conditions.

The proton activation reaction $^{18}O\ (p,n)\ ^{18}F$ has been developed quantitatively by the authors [72] to study oxygen diffusion in polycrystalline beryllium oxide. This technique was first used by Condit [68] who produced autoradiographs from the positron activity of the ^{18}F, as an illustration of grain boundary diffusion in MgO crystals. Similar studies have since been done by McKenzie [69] and Doeffler [73].

The method [72] is illustrated schematically in Figure 12. Beryllium oxide compacts were annealed in contact with a source of ^{18}O, which was either BeO, or CO_2, enriched in ^{18}O. The surface was then ground at a small angle such that the ^{18}O concentration gradient within the sample was exposed.

This surface was irradiated with protons from a 3 MeV Van de Graaff linear accelerator, this machine having the advantage that irradiation conditions are reproducible and stable. The beam energy was calibrated from the ^{18}O (p,n) ^{18}F resonance prior to each experiment by measuring the neutron yield from an enriched $Zr(^{18}O)_2$ target, and was found to be reproducible to within ± 15 keV. The proton beam current was automatically controlled to within a few per cent, and the integrated current recorded for each irradiation. The target assembly was constructed to ensure uniform irradiation of the BeO surface, by oscillation of the sample in the proton beam. Typical operating conditions were: proton current 2 μs at 2.75 MeV, integrated proton current 3000 μ coulomb, pressure 10^{-4} to 10^{-5}mm Hg.

The short-lived γ activity was allowed to decay before proceeding with autoradiographic exposures. The images produced were then examined by means of a microphotometer, from which image density profiles similar to those in Figure 13 were obtained. The response of the film used was found to be closely described by the Beer-Lambert law. However, it was necessary to correct the profiles for broadening due to the range of the 0.635 MeV positrons, and the microphotometer slit width.

The results obtained were analysed on the assumption that the activity of ^{18}O at the surface was effectively constant during the anneal. Diffusion coefficients were calculated from the appropriate solution to Fick's Law for these boundary conditions, and the results at 1400, 1500, and 1900°C are illustrated in Figure 14, for comparison with the previous values obtained by Austerman[66] and Holt[64]. Austerman's data were also obtained for polycrystalline compacts and appear to be in reasonable agreement with this work.

5. SUMMARY

Diffusion mechanisms in ceramic oxides have been discussed and the data available in the literature reviewed. A simple correlation for cation self-diffusion in oxides, based on structural considerations, is not likely to eventuate. For oxygen self-diffusion, however, a correlation should be possible. Some regularity in activation energies in hexagonal, cubic and tetragonal oxides and in the value of diffusion coefficients at the melting point is suggested.

Experimental techniques in the past have been restricted to conventional methods used in the study of diffusion in metals. Greater sensitivity is required as well as better characterization of the materials used. Less common methods for the study of diffusion in oxides have been reviewed.

6. REFERENCES

1. G.C. Kuczynski, (1949). – Trans. A.I.M.E., 185:169.

2. W.D. Kingery and M. Berg, (1955). – J. Appl. Phys., 26:1206.

3. K.D. Reeve, (1966). – AAEC/TM334.

4. C. Wagner, (1951). – Atom Movements, American Society for Metals, p.153.

5. G.W. Castellan and J.W. Moore, (1949). – J. Chem. Phys., 17:41.

6. R. Lindner, (1952). – Acta Chem. Scand., 6:468.

7. R. Lindner, (1952). – Arkiv. Kemi, 4:26.

8. R. Lindner, (1952). – Acta Chem. Scand., 6:457.

9. R.W. Reddington, (1952). – Phys. Rev., 87:1066.

10. R. Haul, L.H. Stein, and J.W.L. de Villiers, (1953). – Nature, 171:619.

11. For example,

(a) W. Jost, (1952). – Diffusion in Solids, Liquids, Gases. Academic Press, New York.

(b) P.G. Shewman, (1963). – Diffusion in Solids. McGraw-Hill, New York.

(c) R. Barrer, (1951). – Diffusion in and Through Solids. Cambridge.

(d) L.A. Girifalco, (1964). – Atomic Migration in Crystals. Blaisdell Publishing Company, New York.

12. For example,

(a) R.E. Howard and A.B. Lidrard, (1964). – Matter Transport in Solids. Rept. Progr. Phys., 27, 161.

(b) A.D. Le Claire, (1964). – Diffusion and Thermal Defects in Solids, in High Temperature Technology. Butterworths, London.

(c) C.E. Birchenall, (1963). – Diffusion in Ionic Crystals, in Physics and Chemistry of Ceramics, Symposium held at Pennsylvania State University. Gordon and Breach, New York.

(d) J.P. Borel, (1966). – La Diffusion dans les Solides. Phys. Stat. Solidi, 13:3.

13. C. Zener, (1952). – Imperfections in Nearly Perfect Crystals, p.289. John Wiley, New York.

14. S. Glasstone, K.J. Laidler, and H. Eyring, (1941). – The Theory of Rate Processes, p.197 and p.524. McGraw-Hill, New York.

15. B.C. Harding, (1967). – Phil. Mag. (in press).

16. B.J. Wuensch and T. Vasilos, (1962). – J. Chem. Phys., 36:2917.

17. J. Rungis and A.J. Mortlock, (1966). – Phil. Mag. 14:821.

18. F. Rueda and W. de Keyser, (1961). – J. Appl. Phys. 32:1799.

19. (a) J.C. Fisher, (1951). – J. Appl. Phys. 22:74.

(b) R.T.P. Whipple, (1954). – Phil. Mag. 45:1225.

(c) A.D. Le Claire, (1963). – Brit. J. Appl. Phys. 14:351.

(d) Toshiyo Suzuoka, (1964). – J. Phys. Soc. Japan, 19:839.

(e). H.J. de Bruin, G.M. Watson, and C.M. Blood, (1966). – J. Appl. Phys. 37:4543.

20. H.J. de Bruin, G.M. Watson and J. Rutherford, Unpublished results.

21. (a) L.P. Belykh, An. N. Nesmeyanov, (1950). – Kokl. Akad. Nauk S.S.S.R., 128,(5):979.

(b) L.P. Firsova, (1959). – Measurement of the Vapour Pressure of Oxides of Li, Be, B, Si and Pb, Dissertation Moscow State University.

(c) O. Kubaschewski and E.L. Evans, (1959). – Metallurgische Thermochemie. V.E.B. Verlag Technik, Berlin.

(d) G. Drummond and R.F. Barrow, (1951). – Trans. Faraday Soc., 98,(3):83.

(e) B.D. Pollock, A.M. Saul, and T.A. Milne, (1960). – The Vaporization of Beryllium Oxide, U.S. Report NAA-SR-3727.

22. E.A. Aitken, (1960). – J. Amer. Ceram. Soc. 43:627.

23. (a) R. Darras, (1965). – Ind. Atom (3u):69.

(b) F. Vodopivec, (1963). – Metanx Corros. Ind., 38:159.

(c) R. Lindner, (1958). – 2nd Intern. Conf. Peaceful Uses of Atomic Energy, 20:116.

24. P.A. Cumming and P.J. Harrop, (1965). – AERE-Bib 143.

25. C.V. Kidson and R. Ross, (1958). – Radioisotopes in Scientific Research, Vol. I p.185, Pergamon Press, New York.

26. D. Lazarus, (1960). – Solid State Physics, 10:71.

27. R. Lindner, (1952). – Proc. Intern. Symp. Reactivity of Solids, Gothenburg, p.195.

28. J. Bernard and J.F. Laurent, ibid,p.577.

29. A.D. Le Claire, (1953). – Pwgr. Metal Phys. 4:265.

30. Y. Oishi and W.D. Kingery, (1960). – J. Chem. Phys. 33:480.

31. (a) S.B. Austerman, (1964). – J. Nucl Mat. 14:248.

(b) J.B. Holt, (1964). – J. Nucl. Mat. 11:107.

32. B.A. Thompson and R.L. Strong, (1963). – J. Phys. Chem., 67:594.

33. Y. Oishi and W.D. Kingery, (1962). – J. Chem. Phys., 36:1383.

34. M. O'Keeffe and W.J. Moore, (1961). – J. Phys. Chem., 65:1438.

35. (a) E.W. Sucov, (1963). – J. Amer. Ceram. Soc., 46:14.

(b) E.L. William, (1963). – J. Amer. Ceram. Soc., 46:190.

36. R. Haul and G. Duembgen, (1965). – Phys. Chem. Solids, 26:1.

37. R. Lindner and A. Akerström, (1965). – Z. Physik. Chem., 6:162.

38. J.M. Fedorchenko and Y.B. Ermolovich, (1960). – Ukrain. Chim. Zhurn., 26:429.

39. D.V. Ignatov, I.N. Belokunova and J.N. Belganin, (1958). – Conference on the use of Radioactive and Stable Isotopes and Radiation in the National Economy and in Science. Proceedings p.326. U.S. Report NP-Er-448 p. 256.

40. S.N. Kryukov and A.A. Zhukhovilzky, (1953). – Dokl. Akad. Nauk S.S.S.R., 90:379, USAEC Translation NSF-tr-77.

41. A.V. Savitsky, (1963). – Phys. Metal. Metall. 16 (6):77.

42. A.A. Zhukhovitsky and A.Y. Geodakyan, (1955). – Zhurn. Fiz., Khimii, 29 (7):1334.

43. H.J. de Bruin and G.M. Watson, (1964). – J. Nucl. Mat. 14:239.

44. H.J. de Bruin and J.W. Kelly, unpublished data.

45. A. Gainotti and L. Zecchina, (1965). – Nuovo Cimento, XLB, 295.

46. P.L. Gruzia and D.F. Litvin, (1955). – Problemy Metallovedeniya i Fizika Metalov, Metallurgizdat, Moscow.

47. A.A. Zhukhovitzky and V.A. Geodakyan, (1955). – Dokl. Akad. Naut, S.S.S.R., 102:301.

48. (a) A.A. Zhukhovitzky, (1959). – J. Appl. Rad. Isotopes, 5:159.

(b) A. Gainotti and L. Zecchma, (1966). – Energia Nucleare, 13(1):32.

49. (a) J.G. Mullen, (1961). – Phys. Rev. 124:1723.

(b) J.G. Mullen, (1962). – Phys. Rev. Letters, 9:383.

50. (a) K. Compaan and Y. Haven, (1956). – Trans. Faraday Soc. 52:786.

(b) K. Compaan and Y. Haven, (1958). – Trans. Faraday Soc., 54:1498.

51. (a) J. Bardeen and C. Herrong, (1951). – Atom Movements, American Society for Metals, p.87.

(b) A.D. Le Claire, (1949). – Progress in Metal Physics, Vol. I,Ch. 7. Pergamon Press, London.

(c) A.D. Le Claire, (1953). – Progress in Metal Physics Vol. 4,Ch. 6. Pergamon Press, London.

(d) A.H. Schoen, (1958). – Phys. Rev. Letters, 1:524.

52. L.W. Barr and A.D. Le Claire, (1964). – Proc. Brit. Ceram. Soc., (1) July: 109–128.

53. A.D. Smiegelskas and E.O. Kirkendall, (1947). – Trans. A.I.M.E. 171:130.

54. (a) L. Boltzmann,(1894). – Ann. Physik. 53:959.

(b) G. Mataro, (1933). – Japan, J. Phys. 8:109.

55. L.D. Hall, (1953). – J. Chem. Phys. 21:87.

56. L.S. Darken, (1948). – Trans. A.I.M.E. 175:184.

57. (a) R.H. Condit and J.B. Holt, (1964). – J. Electrochem. Soc. 111:1192.

(b) J.B. Holt and R.H. Condit, (1966). – Oxygen-18 Diffusion in Surface Defects on MgO as Revealed by Proton Activation, in Materials Science Research Vol. 3, Ch. 2. Plenum Press.

58. B. Cox and C. Roy, (1966). – Electrochem. Techn., 4:121.

59. R.W. Ollerhead, E. Almquist and J.A. Kuchner, (1966). – J. Appl. Phys., 37:2440.

60. R.H. Condit and J.B. Holt, (1965). – Reactivity of Solids, 5th Int. Symposium, Munich, 1964, p.334. Elsevier Publishing Co., Amsterdam.

61. L.C. Northcliffe, (1963). – Ann. Rev. Nucl. Sci., 13:67.

62. G. Friedlander and J.W. Kennedy, (1955). – Nuclear and Radiochemistry. John Wiley and Sons Inc., New York.

63. R. Haul, D. Just and G. Dümbgen (1961). – Reactivity of Solids, Proceedings of the 4th Int. Symposium on the Reactivity of Solids, Amsterdam May 30 to June 4, 1960, p.65. Elsevier Publishing Co., Amsterdam.

64. J.B. Holt, (1964). – J. Nucl. Mat. 11:107.

65. R.H. Condit, Private communications.

66. S.B. Austerman, (1964). – J. Nucl. Mat. 14:248.

67. Ajzenberg – Selove and Lauritsen, (1959). – Nuclear Physics, 11:1.

68. J.B. Holt and R.E. Condit, (1965). – UCRL-7938.

69. D.R. McKenzie, A.W. Searcy, J.B. Holt and R.H. Condit, (1966). – UCRL-14215.

70. A. Choudbury, D.W. Palmer, G. Amsel, H. Curren and P. Baruch, (1965). – Solid State Comm. 3:119.

71. Bing Kwong Mak, J.K. Bird and T.M. Sabine, (1966). – Nature, 211:738.

72. H.J. de Bruin, D.H. Bradhurst and J.W. Kelly, (1967). – Australian and New Zealand Association for the Advancement of Science, 39th Congress, Section B, Melbourne.

73. W.W. Doeffler, (1965). – AECL –2427.

TABLE 1

DIFFUSION OF CHROMIUM IN CHROMIC OXIDE

D_o (cm^2/sec)	Q (kcal/mole)	Reference
4×10^3	100	9
0.137	61.1	10
4.3×10^{-8}	22	11

TABLE 2

POSSIBLE ISOTOPES FOR DETERMINING CATION DIFFUSION MECHANISMS IN CERAMIC OXIDES BY ISOTOPE EFFECTS

Isotope	Half-life	Mode of Decay *	Energy of Major Decay	$(m_2/m_1)^{1/2}-1$	Isotope	Half-life	Mode of Decay *	Energy of Major Decay	$(m_2/m_1)^{1/2}-1$
^{131}Ba	12 d	K(X,γ)	0.496 γ	0.034	^{55}Fe	2.7 y	K(X)	X	0.036
^{140}Ba	12.8 d	$B^-(\gamma)$	1.02 β		^{59}Fe	45 d	$\beta^-(\gamma)$	0.46 β	
^{7}Be	53 d	K(X,γ)	0.48 γ	0.195	^{59}Ni	8×10^4 y	K(X)	X	0.033
^{10}Be	2.7×10^6 y	β^-	0.56 β		^{63}Ni	125 y	β^-	0.067 β	
^{109}Cd	1.3 y	K(X,γ)	0.088 γ	0.027	^{113}Sn	118 d	K(X,γ)	0.255 γ	0.030/0.052
^{115m}Cd	43 d	$\beta^-(\gamma)$	1.61 β		^{121}Sn	27 h	$\beta^-(\gamma)$	0.42 β	
^{139}Ce	140 d	K(X,γ)	0.166 γ	0.020	^{125}Sn	9.4 d	$\beta(\gamma)$	2.34 β	
^{144}Ce	285 d	$\beta^-(\gamma)$	0.134 γ, 0.31 β		^{85}Sr	64 d	K(X,γ)	0.510 γ	0.029
^{56}Co	77.2 d	$\beta^+(\gamma)$	1.46 β, 0.85 γ	0.035	^{90}Sr	28 y	β	0.54 β	
^{60}Co	5.27 y	$\beta^-(\gamma)$	0.31 β, 1.33 γ		^{65}Zn	246 d	K(X,γ) β^+	1.12 γ	0.030
^{68}Ge	280 d	K(X)	1.89 β**	0.022	^{69m}Zn	14 h	γ	0.44 γ	
^{71}Ge	11 d	K(X)	X		^{89}Zr	3.29 d	K(X,γ) β^+	0.90 β, 1.7 γ	0.032/0.043
					^{95}Zr	65 d	β, γ	0.4 β, 0.72 γ	
					^{97}Zr	17 h	β, γ	1.91 β, 0.50 γ	

* K(X,γ) decay by K capture with emission of X-rays and γ radiation.

$\beta(\gamma)$ decay by β emission, secondary γ emission.

** β ex Ga daughter 11 h ^{77}Ge is also available.

TABLE 3

NUCLEAR REACTIONS OF OXYGEN-16

Reaction	Q Value	Reaction	Q Value
$^{16}O\ (\gamma,n)^{15}O$	−15.655	$^{16}O\ (\alpha,\gamma)^{20}Ne$	4.753
$(\gamma,p)^{15}N$	−12.113	$(\alpha,n)^{19}Ne$	−12.158
$(\gamma,t)^{13}N$	−25.020	$(\alpha,p)^{19}F$	−8.119
$(\gamma,\alpha)^{12}C$	−7.148	$(\alpha,pn)^{18}F^*$	−18.533
$(\gamma,n\alpha)^{11}C$	−25.870	$(\alpha,t)^{17}F$	−19.217
$(\gamma,4\alpha)$	−14.429	$(\alpha,{}^3He)^{17}O$	−16.436
$^{16}O\ (d,\gamma)^{18}F^*$	7.538	$^{16}O\ (p,\gamma)^{17}F$	4.984
$(d,n)^{17}F$	−1.631	$(p,n)^{16}F$	−16.41
$(d,p)^{17}O$	1.919	$(p,2p)^{15}N$	−12.113
$(d,t)^{15}O$	−9.396	$(p,d)^{15}O$	−13.428
$(d,{}^3He)^{15}N$	−6.619	$(p,{}^3He)^{14}N$	−15.235
$(d,\alpha)^{14}N$	3.116	$(p,\alpha)^{13}N$	−5.208
$^{16}O\ (n,\gamma)^{17}O$	4.146	$^{16}O\ ({}^3He,n)^{18}Ne$	−2.966
$(n,2n)^{15}O$	−15.655	$({}^3He,p)^{18}F^*$	2.045
$(n,p)^{16}N$	−9.619	$({}^3He,d)^{17}F$	−4.898
$(n,d)^{15}N$	−9.884	$({}^3He,t)^{16}F$	−15.61
$(n,t)^{14}N$	−14.470	$({}^3He,\alpha)^{15}O$	4.923
$(n,{}^3He)^{14}C^*$	−14.607		
$(n,\alpha)^{13}C$	−2.203		
$^{16}O\ (t,n)^{18}F^*$	1.280		
$(t,p)^{18}O$	3.730		
$(t,d)^{17}O$	−2.113		
$(t,{}^3He)^{16}N$	−10.384		
$(t,\alpha)^{15}N$	7.700		

TABLE 4

NUCLEAR REACTIONS OF OXYGEN–17

Reaction	Q Value (MeV)
$^{17}O(n,p)^{17}N$	−7.93
$(n,\alpha)^{14}C$ *	1.825
^{17}O $(p,\gamma)^{18}F$ *	5.619
$(p,n)^{17}F$	−3.550
$(p,d)^{16}O$	−1.919
$(p,t)^{15}O$	−11.316
$(p,\alpha)^{14}N$	1.197
^{17}O $(d,n)^{18}F$ *	3.392
$(d,p)^{18}O$	5.842
$(d,t)^{16}O$	2.113
$(d,\alpha)^{15}N$	9.812
$(d,^{3}He)^{16}N$	−8.271
^{17}O $(t,n)^{19}F$	7.548
$(t,p)^{19}O$	3.542
^{17}O $(^{3}He,\alpha)^{16}O$	16.432
$(^{3}He,d)^{18}F$ *	0.125
$(^{3}He,t)^{17}F$	−2.785
$(^{3}He,p)^{19}F$	8.313
$(^{3}He,n)^{19}Ne$	4.274
^{17}O $(\alpha,n)^{20}Ne$	0.608
$(\alpha,p)^{20}F$	−5.659
$(\alpha,d)^{19}F$	−10.038
$(\alpha,t)^{18}F$*	−14.194

TABLE 5

NUCLEAR REACTIONS OF OXYGEN-18

Reaction	Q Value (MeV)	Reaction	Q Value (MeV)
$^{18}O\ (\gamma,p)^{17}N$	−15.99	$^{18}O\ (t,n)^{20}F$	6.085
		$(t,d)^{19}O$	−2.301
$^{18}O\ (n,\gamma)^{19}O$	3.958	$(t,\alpha)^{17}N$	3.82
$(n,d)^{17}N$	−13.77		
$(n,t)^{16}N$	−13.349	$^{18}O\ (^{3}He,n)^{20}Ne$	13.117
		$(^{3}He,p)^{20}F$	6.850
$^{18}O\ (p,\gamma)^{19}F$	7.964	$(^{3}He,d)^{19}F$	2.470
$(p,n)^{18}F\ *$	−2.450	$(^{3}He,t)^{18}F\ *$	−1.685
$(p,d)^{17}O$	−5.842	$(^{3}He,\alpha)^{17}O$	12.509
$(p,t)^{16}O$	−3.730		
$(p,{}^{3}He)^{16}N$	−14.114	$^{18}O\ (\alpha,n)^{21}Ne$	−0.705
$(p,\alpha)^{15}N$	3.970	$(\alpha,d)^{20}F$	−11.501
		$(\alpha,t)^{19}F$	−11.849
$^{18}O\ (d,n)^{19}F$	5.737	$(\alpha,{}^{3}He)^{19}O$	−16.620
$(d,p)^{19}O$	1.731		
$(d,t)^{17}O$	−1.810		
$(d,{}^{3}He)^{17}N$	−10.50		
$(d,\alpha)^{16}N$	5.737		
$(d,2n)^{18}F\ *$	−4.67		

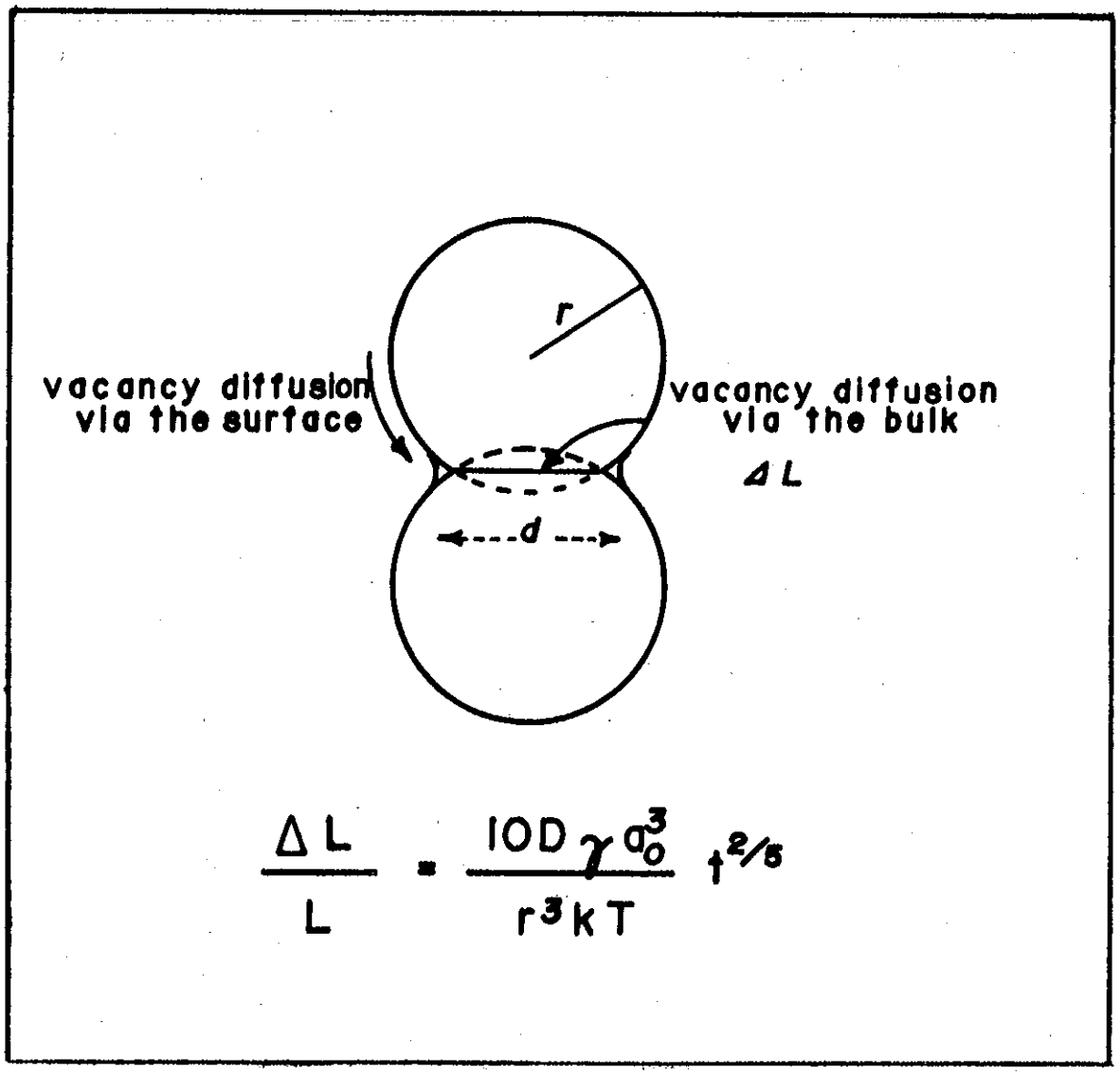

FIGURE 1. SINTERING MODEL ACCORDING TO KINGERY AND BERG

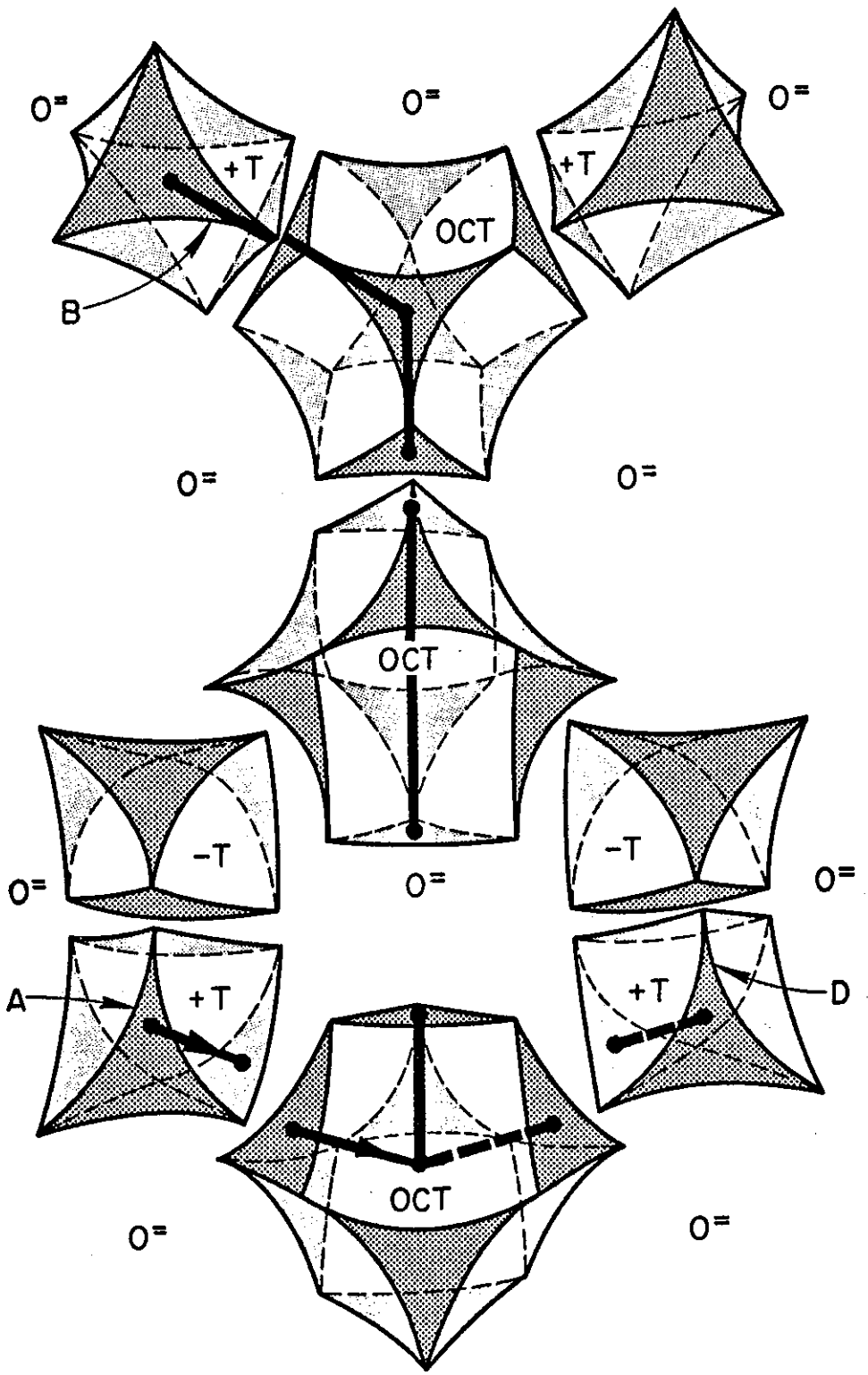

FIGURE 2. EXPLODED VIEW OF INTERIONIC SPACE IN A CLOSEST PACKED HEXAGONAL OXIDE LATTICE

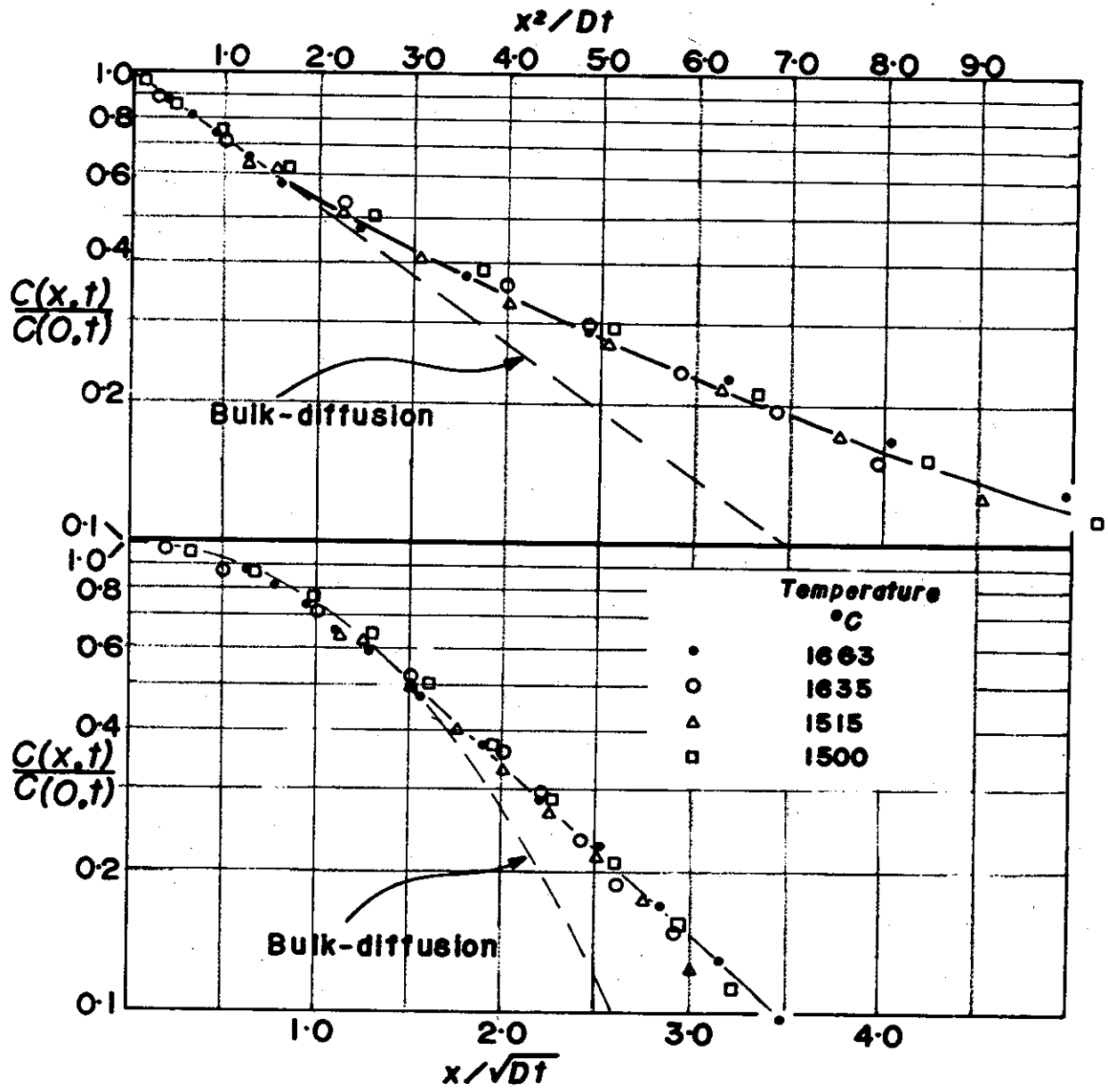

FIGURE 3. PENETRATION PROFILE FOR THE DIFFUSION OF ^{7}Be INTO POLYCRYSTALLINE BeO

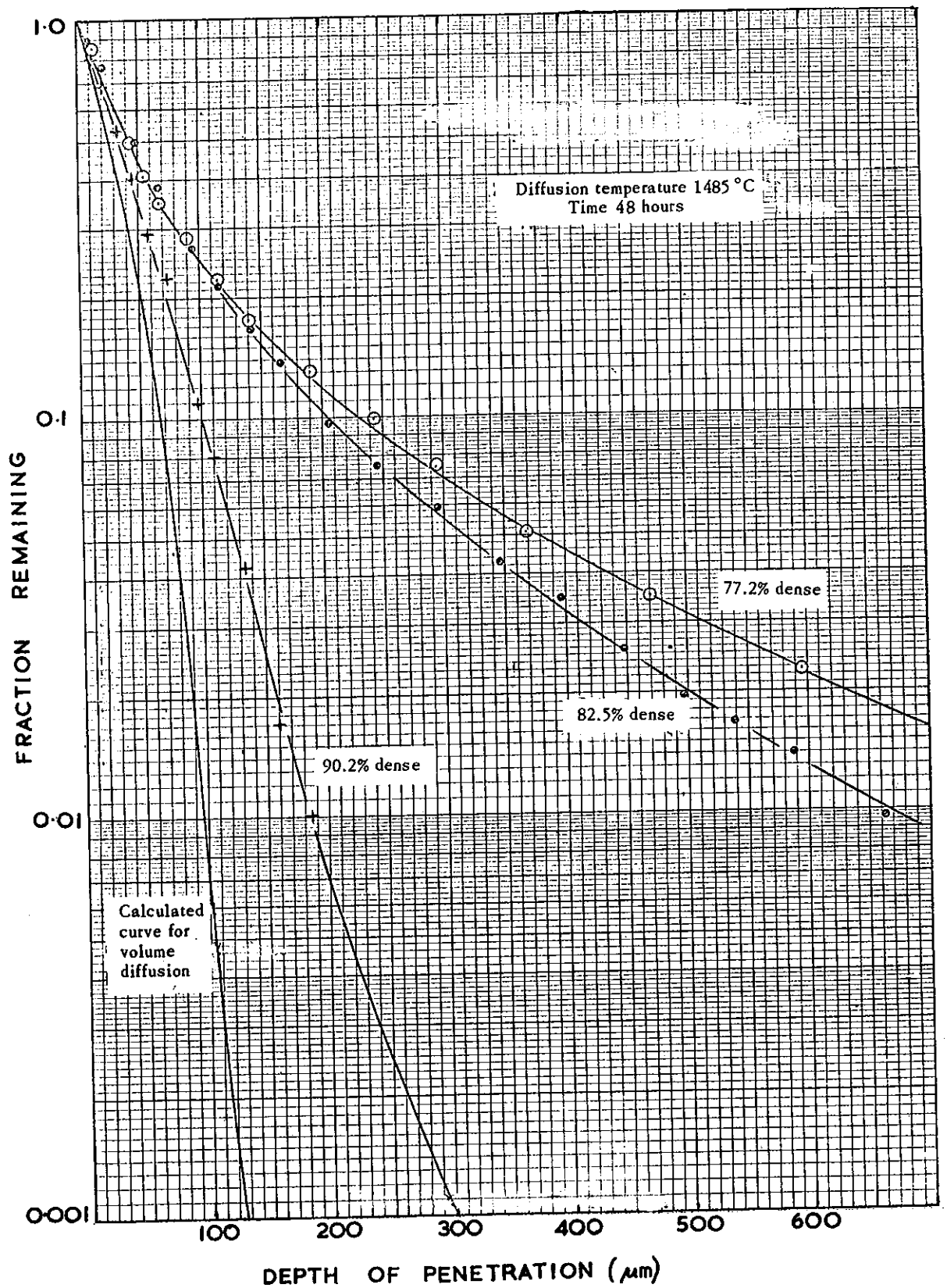

FIGURE 4. CATION SELF-DIFFUSION IN LOW-DENSITY POLYCRYSTALLINE BeO

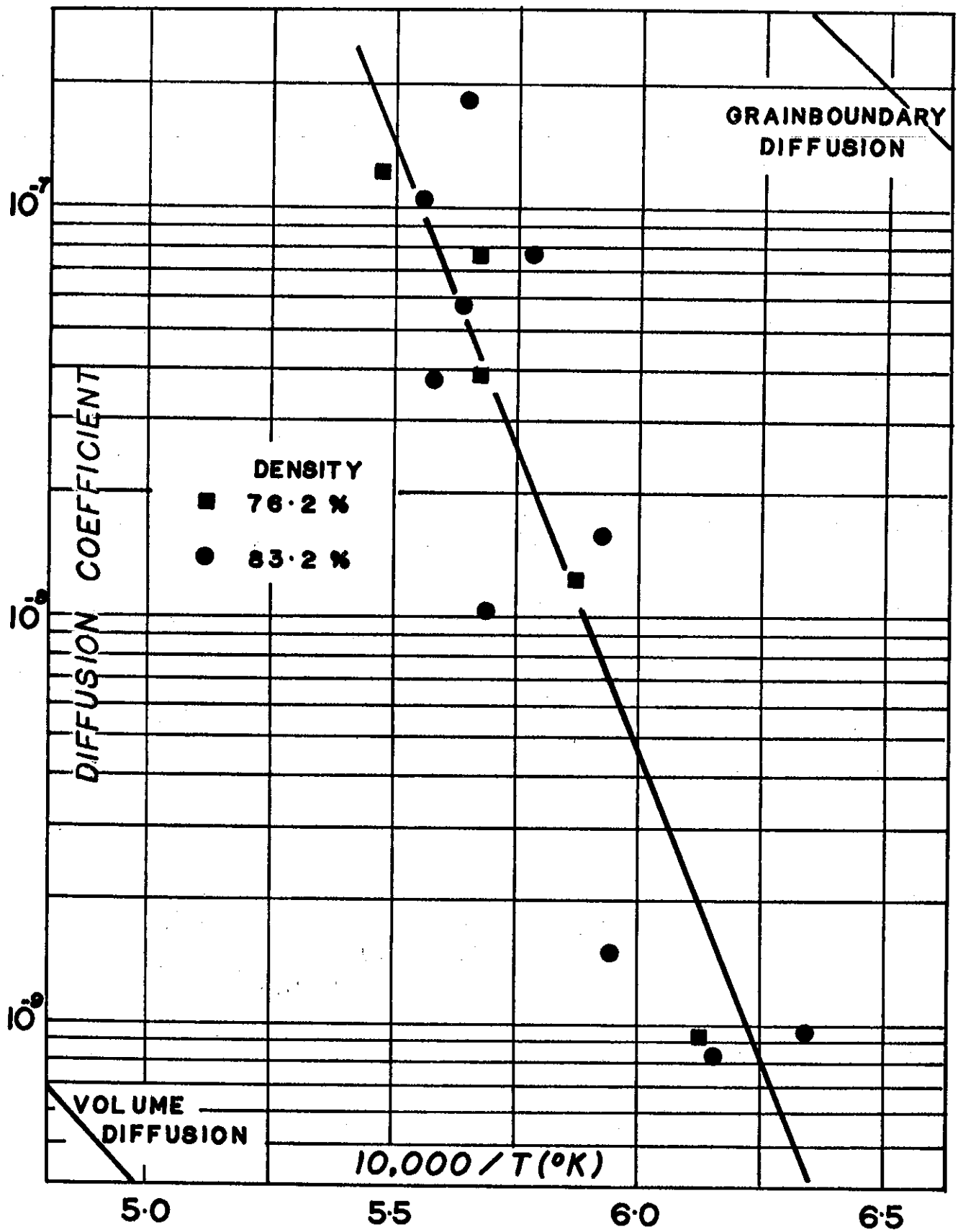

FIGURE 5. COEFFICIENTS FOR INTERGRANULAR DIFFUSION IN LOW DENSITY BeO

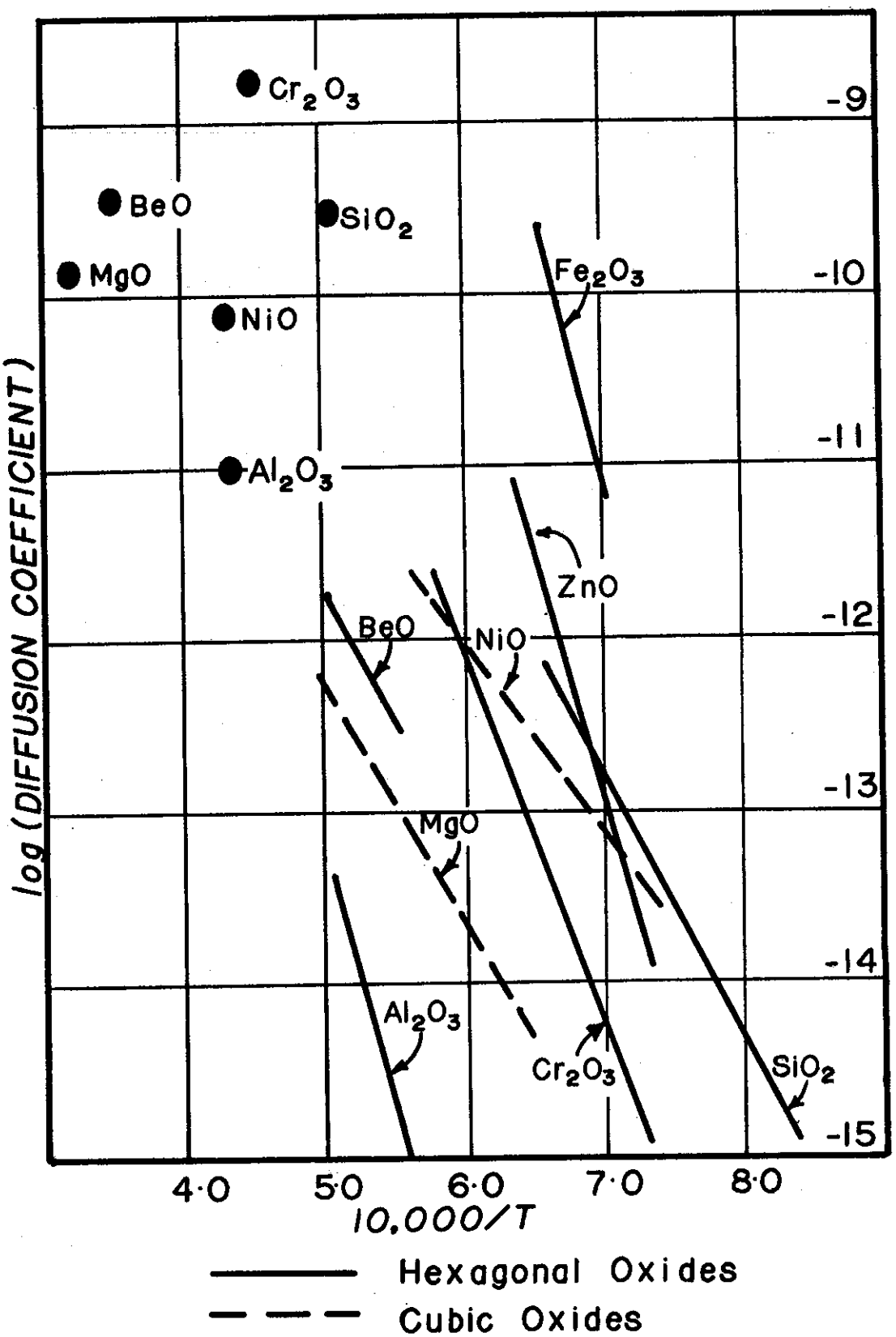

FIGURE 6. OXYGEN DIFFUSION IN CERAMIC OXIDES

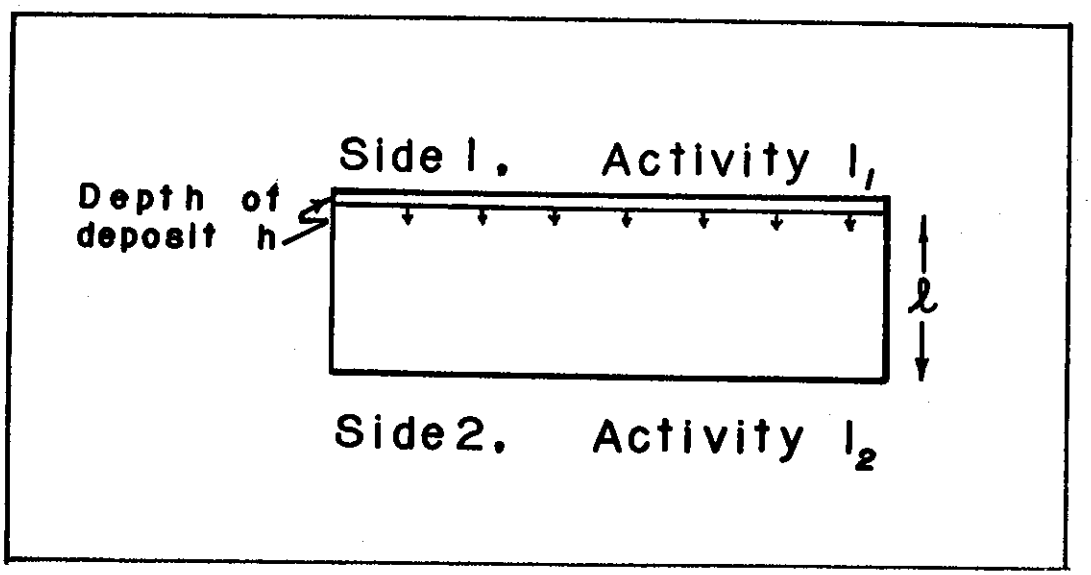

FIGURE 7. ABSORPTION OF SOFT RADIATION DURING DIFFUSION

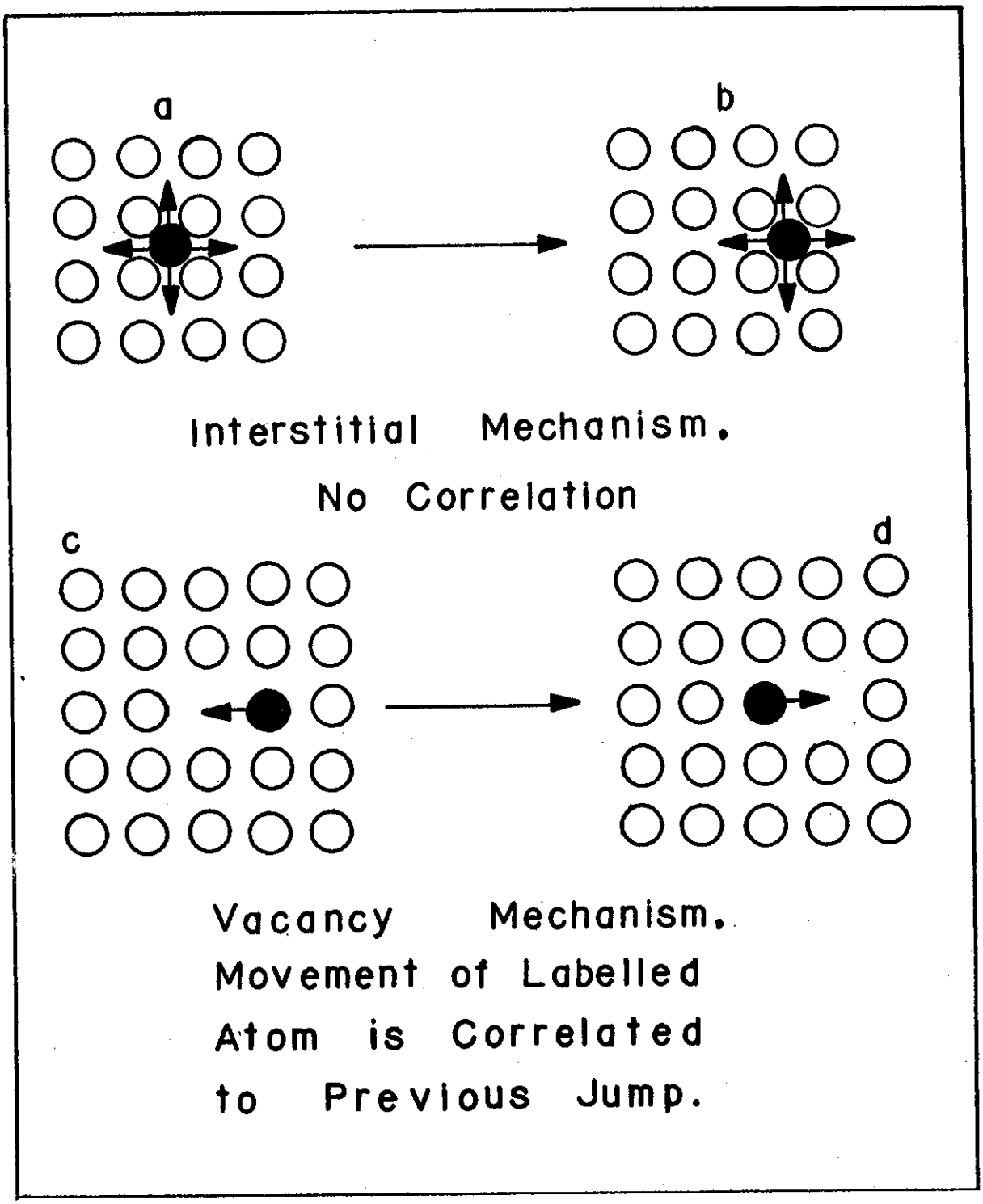

FIGURE 8. BASIC PRINCIPLES OF CORRELATION

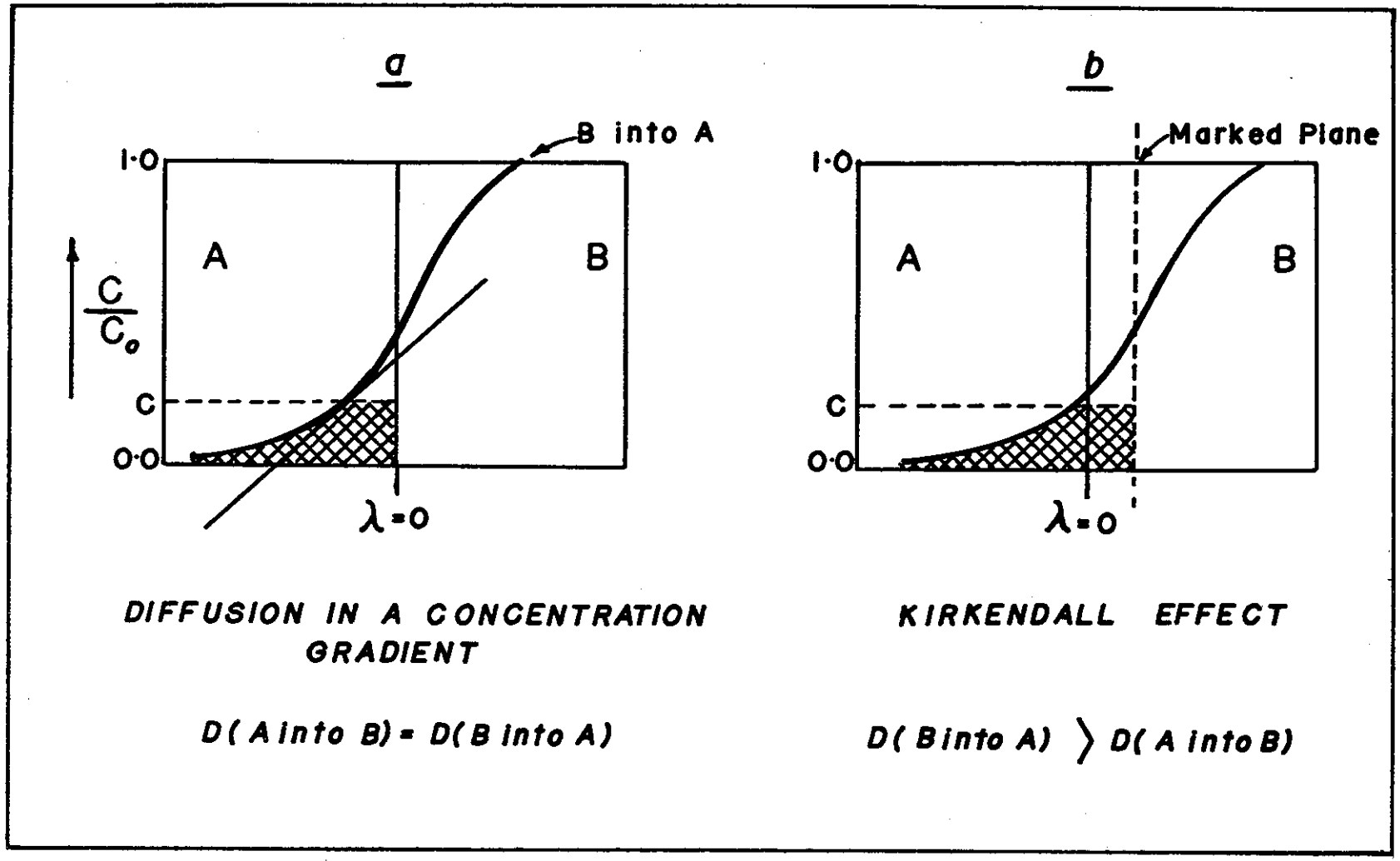

FIGURE 9. CHEMICAL DIFFUSION

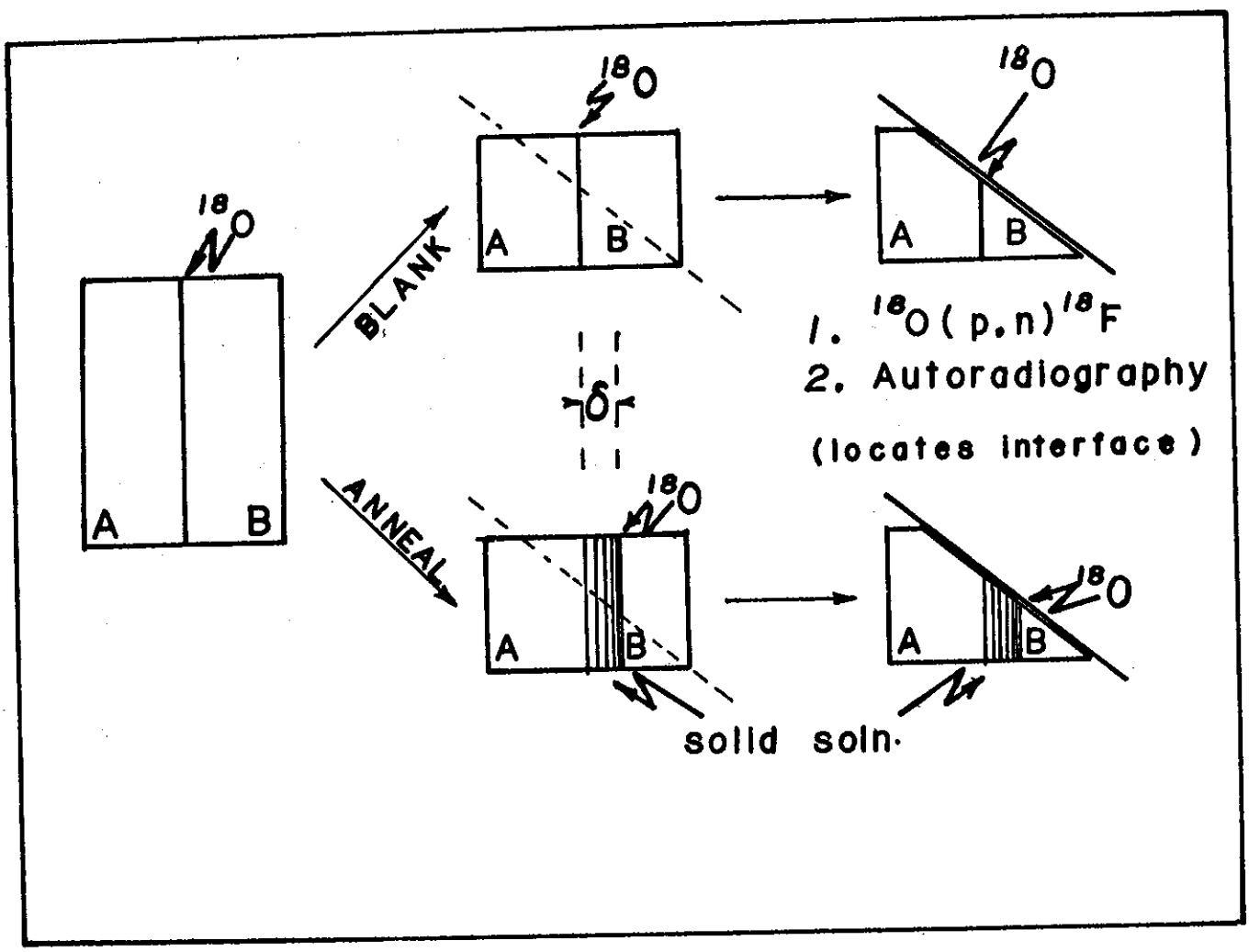

FIGURE 10. ^{18}O MARKER SHIFT IN CHEMICAL DIFFUSION

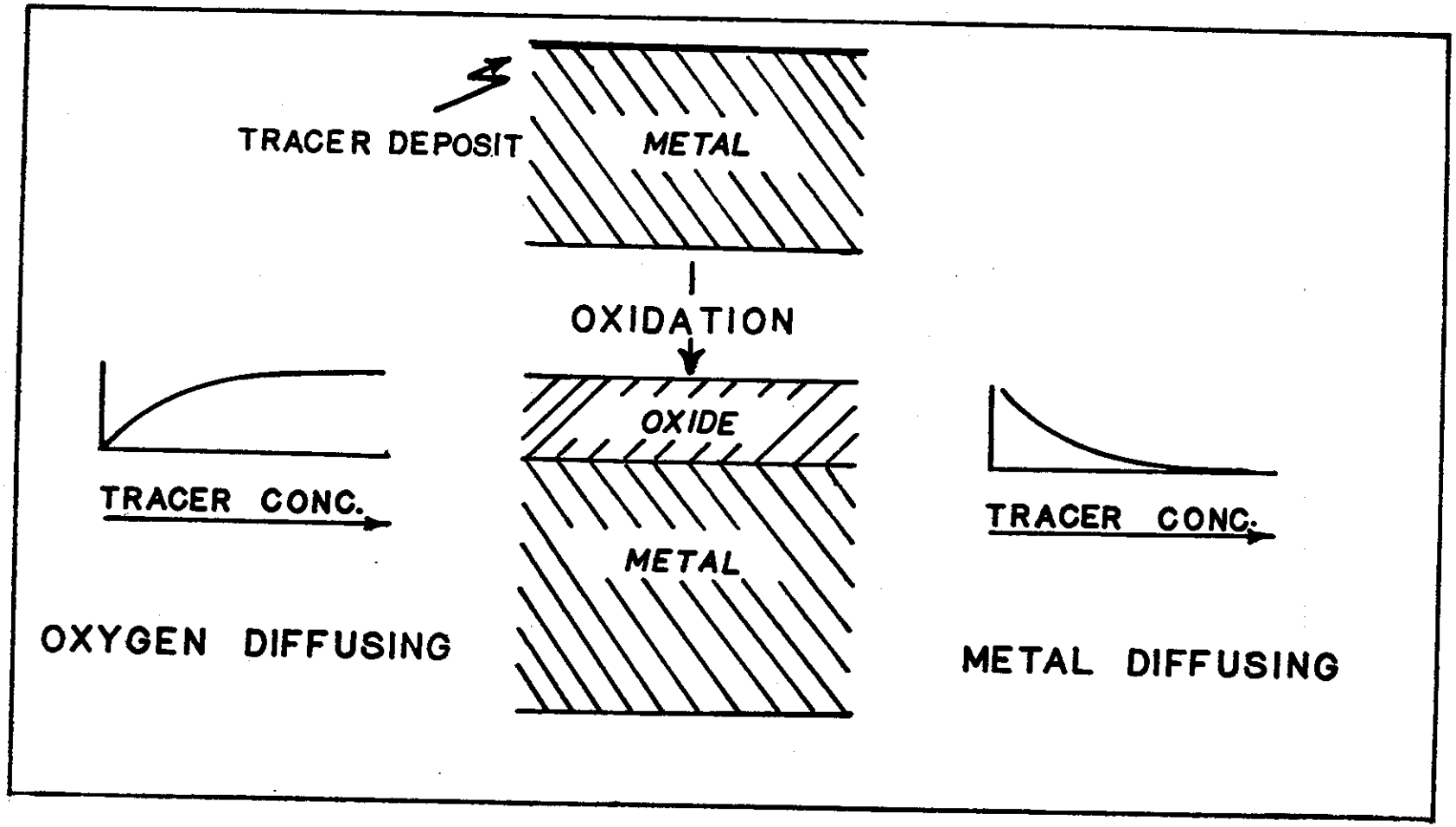

FIGURE 11. METAL OXIDATION. MIGRATION OF METAL TRACER THROUGH OXIDE LAYER

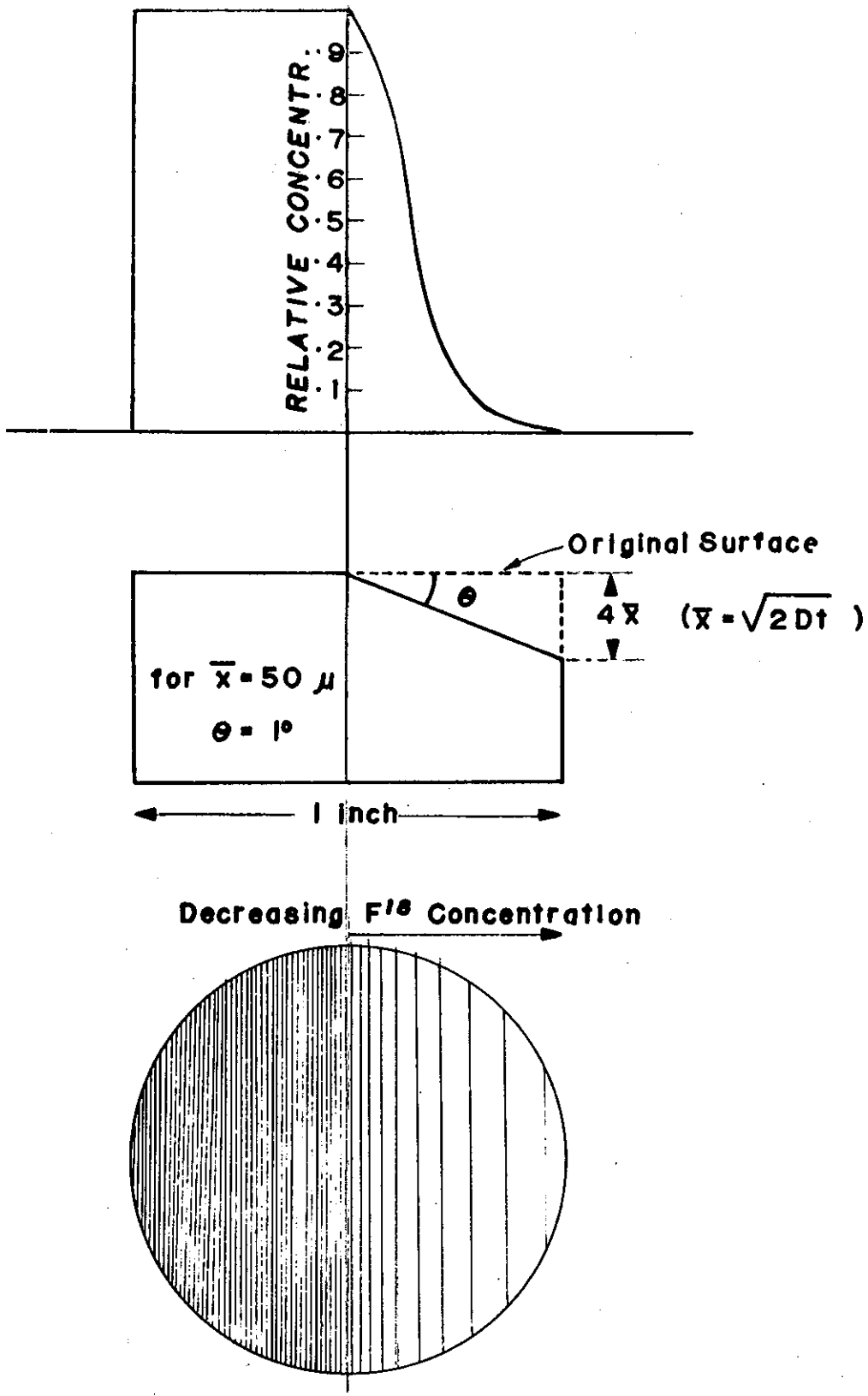

FIGURE 12. EXPERIMENTAL DETERMINATION OF OXYGEN DIFFUSION BY PROTON ACTIVATION OF ^{18}O

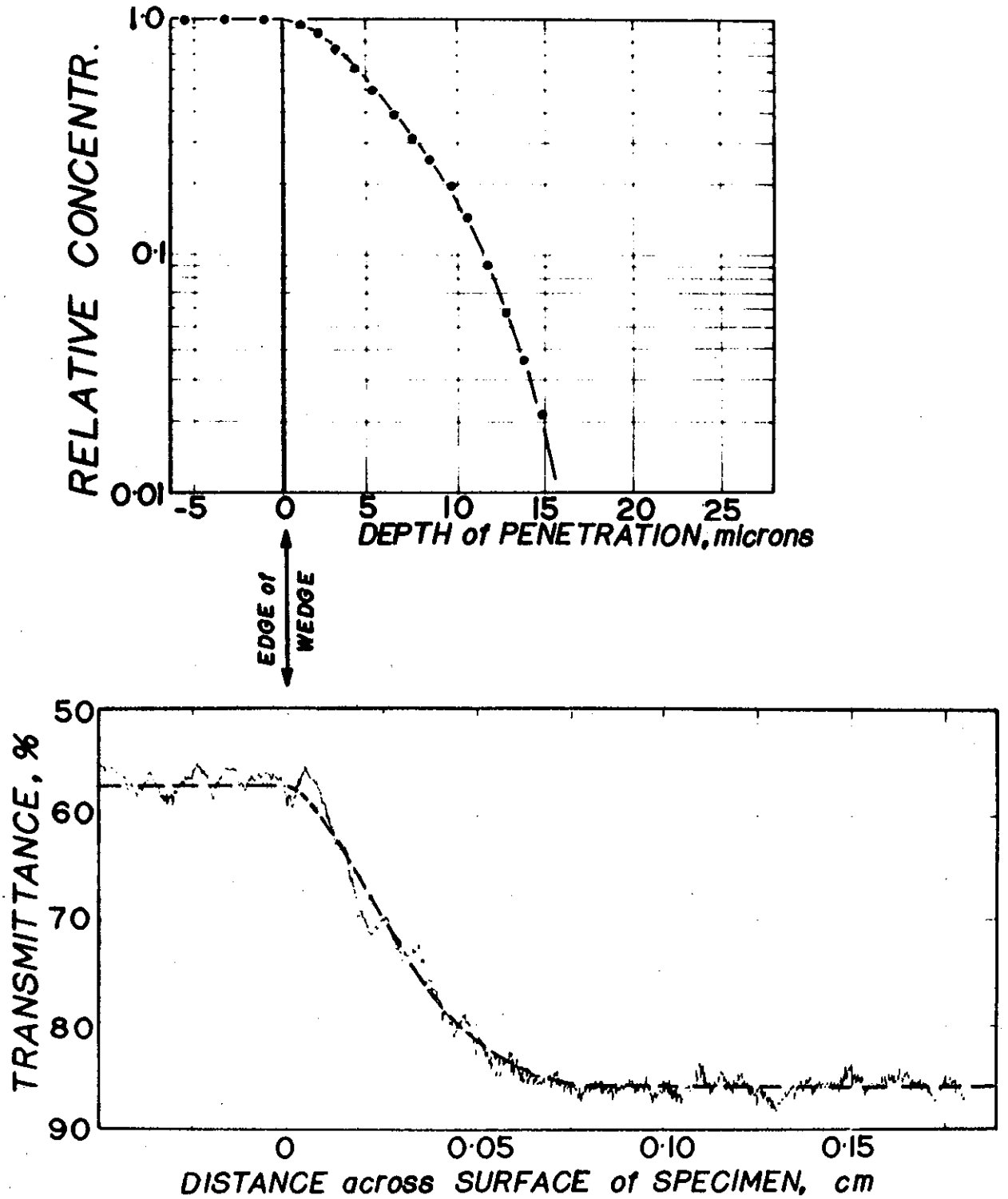

FIGURE 13. MICROPHOTOMETER ANALYSIS OF ^{18}F AUTORADIOGRAPH

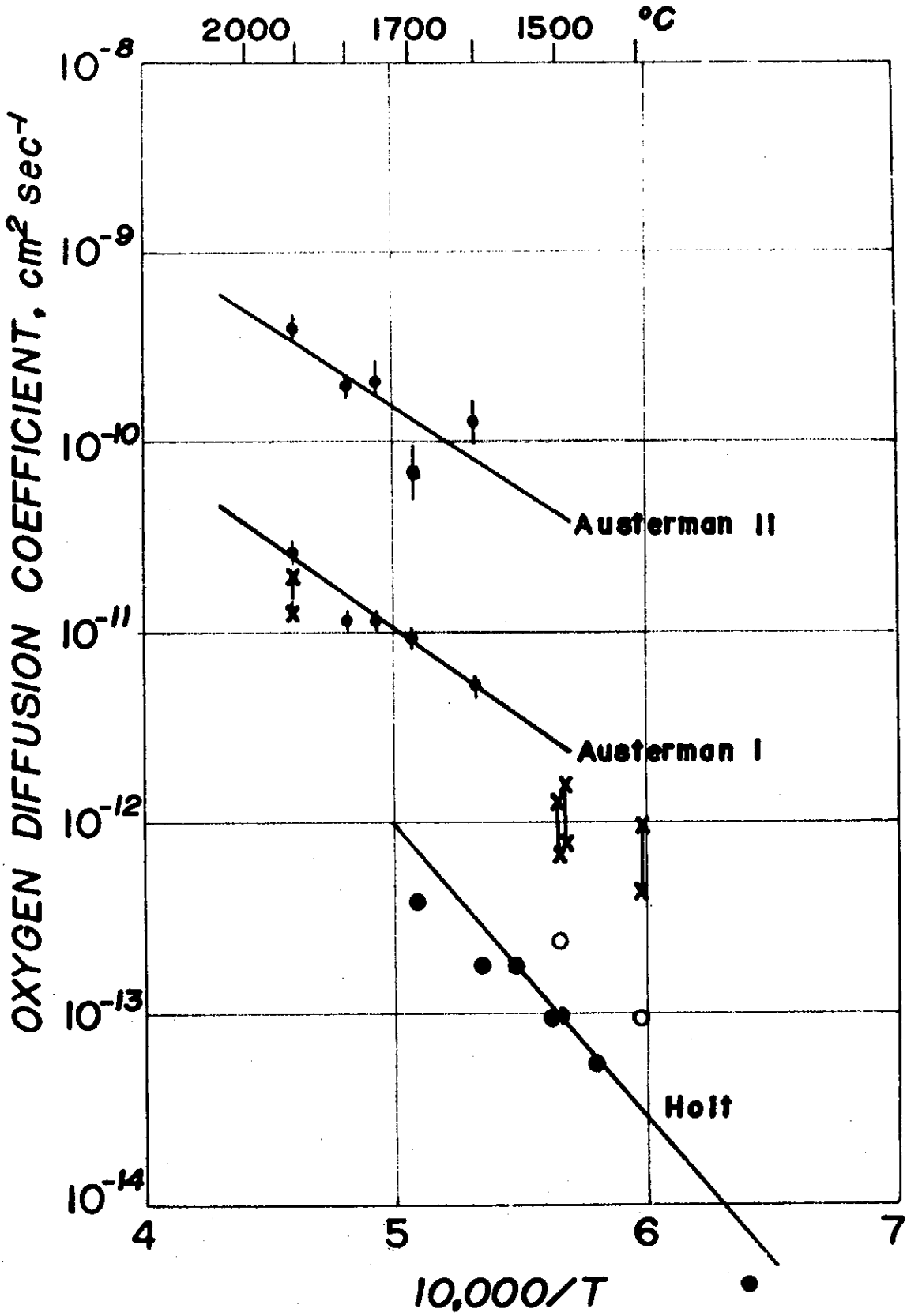

FIGURE 14. OXYGEN DIFFUSION IN BERYLLIUM OXIDE